



UPPSALA
UNIVERSITET

*Digital Comprehensive Summaries of Uppsala Dissertations
from the Faculty of Medicine 1817*

Brain distribution of a bispecific antibody targeting A β

GUSTAVSSON TOBIAS



ACTA
UNIVERSITATIS
UPSALIENSIS
UPPSALA
2022

ISSN 1651-6206
ISBN 978-91-513-1436-5
URN urn:nbn:se:uu:diva-469103

Dissertation presented at Uppsala University to be publicly examined in Fåhraeusalen, Rudbecklaboratoriet, Dag Hammarskjölds Väg 20, Uppsala, Friday, 22 April 2022 at 13:00 for the degree of Doctor of Philosophy (Faculty of Medicine). The examination will be conducted in English. Faculty examiner: Professor Danica Stanimirovic (National Research Council of Canada and University of Ottawa).

Abstract

Tobias, G. 2022. Brain distribution of a bispecific antibody targeting A β . *Digital Comprehensive Summaries of Uppsala Dissertations from the Faculty of Medicine* 1817. 66 pp. Uppsala: Acta Universitatis Upsaliensis. ISBN 978-91-513-1436-5.

Alzheimer's disease (AD) is characterised by aberrant protein aggregation in the brain with subsequent synaptic loss, neuroinflammation, and brain atrophy that ultimately clinically manifests as cognitive impairment. Histopathological findings in AD are extracellular plaques of the protein amyloid-beta (A β), A β in blood vessels (CAA), and intracellular neurofibrillary tangles (NFT) of hyperphosphorylated tau. The FDA recently approved the antibody aducanumab for AD treatment, and several antibodies are now in clinical phase 3 trials, demonstrating that A β -directed immunotherapy is a viable treatment option in AD.

In this thesis we evaluated the therapeutic A β antibodies 3D6 and RmAb158 in comparison with the bispecific RmAb158-scFv8D3, which penetrates the blood-brain barrier (BBB) by transferrin receptor mediated transcytosis. Emphasis lies in antibody brain uptake and intra brain distribution, in their use as potential treatment options in AD and how such treatment affects BBB integrity.

Vascular disturbances are common side effects of anti-A β immunotherapy. However, we demonstrated that the BBB permeability of large molecules is unchanged following acute 3D6 treatment in an A β mouse model (paper I). Next, brain uptake and distribution of radioiodinated RmAb158 and its bispecific variant RmAb158-scFv8D3 were investigated with SPECT in an A β mouse model. Due to its active transport across BBB, RmAb158-scFv8D3 had a higher brain uptake than RmAb158, resulting in greater total brain exposure, and higher concentration at A β plaques (paper II). In paper III, we labelled RmAb158-scFv8D3 with the radiometal indium-111 (¹¹¹In), using chelators CHX-A''-DTPA or DOTA, and SPECT was used to investigate brain retention and biodistribution. The ¹¹¹In-labelled bispecific antibody entered the brain, and although brain retention was higher in A β mice, the wild type (wt) background was high. SPECT revealed high bone uptake of all tracers, and subsequent ex vivo measurement pinpointed retention to the bone marrow. With the knowledge gained from paper II, we addressed whether RmAb158-scFv8D3 would improve treatment efficacy in different treatment regimes. We also assessed the immunogenicity of different antibody constructs upon chronic administration (paper IV). As all tested bispecific antibody constructs elicited a humoral response, immune cell depletion was necessary before repeated antibody treatment. Overall, long-term treatment of RmAb158-scFv8D3 did lower total brain A β but compared with RmAb158, it did not improve treatment efficacy.

In conclusion, acute anti-A β immunotherapy did not negatively affect BBB integrity, and bispecific antibodies displayed improved brain distribution and long-term accumulation at parenchymal A β . However, this did not translate into an added treatment effect in a chronic therapeutic setting.

Keywords: Alzheimer's disease, amyloid-beta, blood-brain barrier, single-photon emission computed tomography (SPECT), bispecific antibody, immunotherapy

Gustavsson Tobias, Department of Public Health and Caring Sciences, Box 564, Uppsala University, SE-75122 Uppsala, Sweden.

© Gustavsson Tobias 2022

ISSN 1651-6206

ISBN 978-91-513-1436-5

URN urn:nbn:se:uu:diva-469103 (<http://urn.kb.se/resolve?urn=urn:nbn:se:uu:diva-469103>)

List of Papers

This thesis is based on the following papers, which are referred to in the text by their Roman numerals.

- I. Gustafsson S, **Gustavsson T**, Roshanbin S, Hultqvist G, Hammarlund-Udenaes M, Sehlin D, Syvänen S (2018). Blood-brain barrier integrity in a mouse model of Alzheimer's disease with or without acute 3D6 immunotherapy. *Neuropharmacology*. 143:1-9
- II. **Gustavsson T**, Syvänen S, O'Callaghan P, Sehlin D (2020). SPECT imaging of distribution and retention of a brain-penetrating bispecific amyloid- β antibody in a mouse model of Alzheimer's disease. *Translational neurodegeneration*. 9(1):37
- III. **Gustavsson T**, Sehlin D, Syvänen S. Indium-111 radiolabeling of a brain-penetrant antibody for in vivo SPECT of brain A β . *Manuscript*
- IV. **Gustavsson T**, Hultqvist G, Metzendorf N, Roshanbin S, Julku U, Nilsson P, Honek K, Laudon H, Syvänen S, Sehlin D. Long-term immunotherapy with bispecific antibodies in a mouse model of Alzheimer's disease. *Manuscript*

Reprints were made with permission from the respective publishers.

List of non-thesis publications

- V. Rofo F, Buijs J, Falk R, Honek K, Lannfelt L, Lilja AM, Metzendorf NG, **Gustavsson T**, Sehlin D, Söderberg L, Hultqvist G (2021). Novel multivalent design of a monoclonal antibody improves binding strength to soluble aggregates of amyloid beta. *Translational Neurodegeneration* 10, 38.
- VI. Rofo F, Ugur Yilmaz C, Metzendorf N, **Gustavsson T**, Beretta C, Erlandsson A, Sehlin D, Syvänen S, Nilsson P, Hultqvist G (2021). Enhanced neprilysin-mediated degradation of hippocampal A β 42 with a somatostatin peptide that enters the brain. *Theranostics* 11, 789–804
- VII. Sehlin D, Stocki P, **Gustavsson T**, Hultqvist G, Walsh FS, Rutkowski JL, Syvänen S (2020). Brain delivery of biologics using a cross-species reactive transferring receptor 1 VNAR shuttle. *FASEB J* 34:13272-13283
- VIII. Syvänen S, Hultqvist G, **Gustavsson T**, Gumucio A, Laudon H, Söderberg L, Ingelsson M, Lannfelt L, Sehlin D (2018). Efficient clearance of A β protofibrils in A β PP-transgenic mice treated with a brain-penetrating bifunctional antibody. *Alzheimer's Research and Therapy*, 10:49

Contents

Introduction.....	9
Alzheimer's disease.....	9
Amyloid beta	10
Tau	13
Barriers of the brain	13
Neuroinflammation.....	17
Diagnostic biomarkers in AD	18
Immunotherapy in Alzheimer's disease	21
Enhancement of antibody brain uptake	23
Brain elimination of therapeutic antibodies.....	25
ImmunoPET imaging with bispecific antibodies.....	26
Anti-drug antibodies	26
Aim	28
Methods	29
Animal models.....	29
Recombinant expression of bispecific antibodies.....	30
Design of antibodies with reduced immunogenicity	30
Radioiodine labelling of antibodies	31
Radiometal labelling of antibodies	31
Real-time measurement of tracer kinetics using Ligandtracer	32
Molecular imaging.....	33
Assessment of BBB permeability	34
Brain tissue processing	34
Autoradiography/emulsion autoradiography	35
Tissue staining	36
Enzyme-linked immunosorbent assay (ELISA)	37
Paper I.....	38
Paper II	39
Paper III	41
Paper IV	43
Conclusion and future perspectives	47
Populärvetenskaplig sammanfattning	49

Acknowledgement51
References.....54

Abbreviations

^{124}I	Iodine-124
^{125}I	Iodine-125
^{111}In	Indium-111
A β	Amyloid-beta
APP	Amyloid precursor protein
AD	Alzheimer's disease
Arc	Arctic mutation in APP
ARIA	Amyloid-related imaging abnormalities
BACE-1	β -amyloid cleaving enzyme-1
BBB	Blood-brain barrier
BCSFB	Blood-cerebrospinal fluid barrier
bsAb	Bispecific antibody
CAA	Cerebral amyloid angiopathy
CHX-A''-DTPA	[(R)-2-Amino-3-(4-aminophenyl)propyl]-trans-(S,S)-cyclohexane-1,2-diamine-pentaacetic acid
CNS	Central nervous system
CSF	Cerebrospinal fluid
DOTA	2,2',2'',2'''-(1,4,7,10-Tetraazacyclododecane-1,4,7,10-tetrayl)tetraacetic acid
ISF	Interstitial fluid
I.V	Intravenous
MCI	Mild cognitive impairment
mTfR	Mouse transferrin receptor
NFT	Neurofibrillary tangle
NVU	Neurovascular unit
PET	Positron-emission tomography
RMT	Receptor-mediated transport
ScFv	Single-chain variable fragment
SPECT	Single-photon emission computed tomography
Swe	Swedish mutation in APP
Tf	Transferrin
TfR	Transferrin receptor
WT	Wild-type

Introduction

Alzheimer's disease

As of 2019, approximately 50 million people worldwide are living with dementia. This number is projected to increase to 150 million people by 2050, and the global economic burden of caring for people with dementia is estimated to rise to 2 trillion USD annually by 2030 [1]. Dementia is not a new concept; during the antiquity the ancient Greeks formulated the idea of dementia. Alois Alzheimer was the first to describe the clinical and histopathological findings in Alzheimer's disease (AD). On November 26, 1901, Alois Alzheimer met Auguste Deter, a patient in a mental asylum in Frankfurt. Clinically, Deter was found to be disoriented and confused, which worsened over time, and after 5 years she died due to sepsis. During *post-mortem* examination of Deter's brain, Alzheimer found the now well-established hallmarks of AD, such as brain atrophy, amyloid plaques and tangles [2].

AD is the leading cause of dementia and is characterised by progressive neurodegeneration that takes decades to develop, resulting in a detrimental effect on cognitive functions such as memory and language. Initial symptoms include a reduction in the ability to form new memories, which subsequently, as the disease progresses, impairs AD patients' ability to retrieve declarative long-term memories [3]. Canonical histopathological findings in the AD brain include extracellular amyloid plaques (senile plaques), composed of insoluble amyloid β ($A\beta$) fibrils, and intraneuronal neurofibrillary tangles (NFTs) formed by hyperphosphorylated tau protein [4]. The pathological processes leading to AD begins to develop decades before symptom onset. Imaging and biomarker studies in AD patients demonstrate a lag period where $A\beta$ accumulates years, or decades, before the onset of clinical symptoms. Amyloid positron emission tomography (PET) and cerebrospinal fluid (CSF) biomarkers indicate that the progressive buildup of $A\beta$ precedes other pathological changes in AD [5].

Amyloid beta

APP processing and A β aggregation

A β is produced by proteolytic processing of the amyloid β precursor protein (APP). The APP gene, located on chromosome 21, can be alternatively spliced into three isoforms, where the 695 amino acid splice variant is the predominant isoform found in neurons [6]. APP is a transmembrane protein consisting of a single transmembrane domain, an extracellular domain, and a cytoplasmic tail. Neuronal APP metabolism can be divided into an amyloidogenic and a non-amyloidogenic pathway (Figure 1). In the amyloidogenic pathway the A β protein is produced via the action of two enzymes: β -site amyloid precursor protein cleaving enzyme-1 (BACE-1), an aspartyl protease, and γ -secretase, an intramembrane enzyme complex including the presenilin proteins. The amyloidogenic pathway starts with cleavage of APP's β -site by BACE-1, generating a 99 residue protein, APP-CTF99, which is further cleaved at its γ -site by the γ -secretase complex. This results in the formation of the approximately 4.5 kDa A β peptide [7, 8], with a length between 38 to 43 amino acids[9].

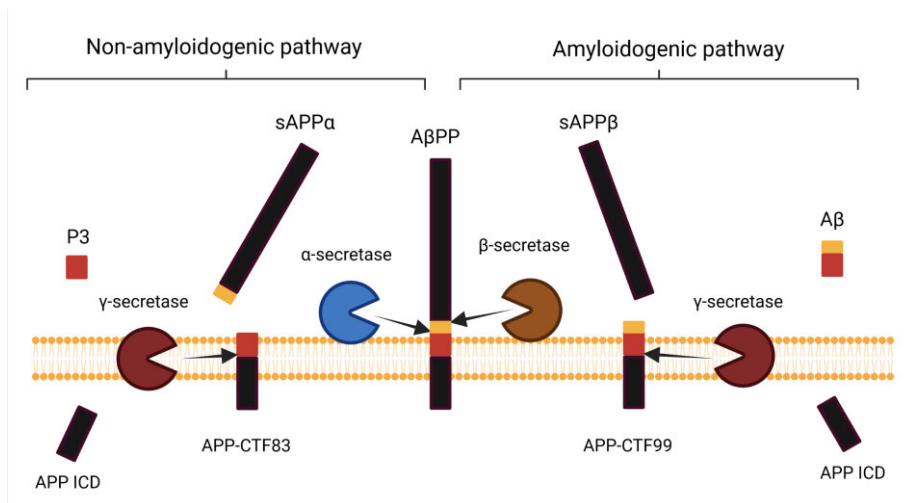


Figure 1. Processing of APP via the (left) non-amyloidogenic and amyloidogenic pathway (right). A β is generated from APP via the action of BACE-1 and the gamma-secretase complex.

Natively, A β is an unstructured protein but it can adopt a β -hairpin motif that promotes the formation of dimers, tetramers, and oligomers that aggregate into protofibrils. The protofibrils can be organised into insoluble fibril structures that aggregate and deposit into plaques (Figure 2) [10].

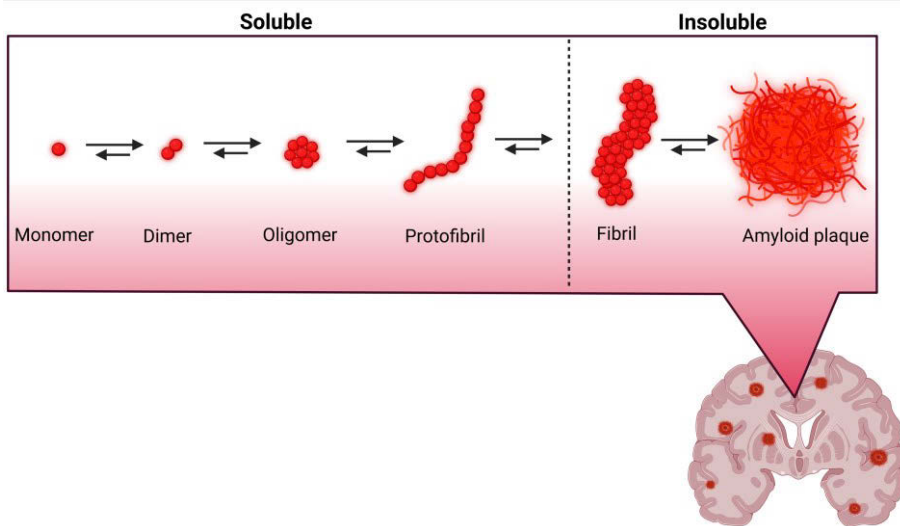


Figure 2. A β aggregation. A β monomers aggregate into larger soluble structures, including oligomers and protofibrils. Continued aggregation forms large insoluble A β amyloid fibrils deposited as plaques in brain.

A β deposition

A β plaque morphology in AD brains are often classified into dense-cored, fibrillary, or diffuse plaques. Dense-cored plaques are characterised by a central mass, surrounded by a void, and an outer spherical shell of A β . Fibrillar plaques present as a dense structure with spoke-like structures emanating from the centre. Diffuse plaques are generally larger, less compact and display a homogenous distribution with no substructures [11]. Examined in detail, A β plaques comprise central core A β fibrils surrounded by a halo of smaller fibrillar and non-fibrillar A β structures [12]. The core is mainly composed of A β 40, whereas A β 42 is the primary A β species found in the surrounding halo [13]. A majority of AD patients display A β -aggregation in blood vessels in the brain, also known as cerebral amyloid angiopathy (CAA)[14], which destabilises the brain vasculature and increases the risk for intracerebral haemorrhage [15, 16]. A β 40 constitutes the majority of amyloid deposits in vessel walls [17, 18], and is thought to reflect the failure of A β clearance into the blood [19].

Normal function and pathological gain-of-function of A β

Much of the research exploring the properties of APP and subsequent generation of A β has focused on the detrimental effects of high A β concentrations in the brain. However, low physiological concentrations of monomeric A β may be beneficial and be involved in several brain functions, such as modulating synaptic activity, enhancing memory formation [20, 21],

and may even have antimicrobial properties that protect the brain from infections [22].

Yet, there is clear evidence of aberrant accumulation and A β -induced toxicity in AD. The amyloid cascade hypothesis states that accumulation of A β in the brain is the main cause of AD, facilitating subsequent pathological changes such as NFT formation and cell loss leading to dementia [23]. Initially, insoluble A β in the form of senile plaques, was considered to be the causative driver in AD pathogenesis, but focus has shifted to soluble oligomeric A β species as the underlying agent of the detrimental effects seen in AD [24]. Supporting this is the general lack of correlation between the cognitive severity of AD and plaque burden [24]. In addition, a pronounced plaque burden is often observed also in the cognitively normal aging population [25]. Instead, soluble oligomeric A β species have adverse effects on neuronal synaptic function [26], impair memory [27], and are toxic to neurons [28].

Clearance of A β from the brain

Normally, A β is cleared by enzymatic degradation or transport out of the brain. A shift favoring accumulation over clearance is believed to contribute to the progressive accumulation of A β over time and AD development.

Zinc metalloproteases are an enzyme class that facilitate A β degradation. These include neprilysin, insulin-degrading enzyme, and matrix metalloproteinases [29]. Neprilysin is located at the cell membrane and its role in A β catabolism has been extensively studied. *In vivo* evidence where neprilysin deficient mice were cross-breed with an A β mouse model, resulted in increased oligomeric A β and cognitive deficits [30]. Furthermore, reduced neprilysin concentration is seen in AD brains [31], highlighting the potential protective role the enzyme typically plays in AD disease progression.

Non-enzymatic A β removal relies on microglial phagocytosis, interstitial fluid bulk flow clearance, and efflux transport over the blood-brain barrier (BBB). Brain-residing phagocytic cells such as microglia [32] and supportive astrocytes [33] have been suggested to remove parenchymal A β through phagocytosis. Other clearance pathways include interstitial fluid (ISF) bulk flow transports A β into cerebrospinal fluid (CSF). Alternatively, A β in ISF is transported via perivascular pathways to the subarachnoid space where A β is taken up in cervical lymph nodes. P-glycoprotein 1 (ABCB1) and low-density lipoprotein receptor-related protein 1 (LRP1), both located at the BBB, are transport proteins facilitating A β efflux. ApoE plays a central role in this system, in which A β bound to ApoE is transported by these receptors across the BBB to the blood circulation [34].

Genetics in Alzheimer's disease

Sporadic, or late-onset AD, is the most common form of the disease, and accounts for >95% of all new AD cases. However, familial causes of AD (FAD) have been discovered that lead to early onset of the disease. The majority of the mutations are found in the APP gene or in the *PSEN1* and *PSEN2* genes [35], which encode presenilin proteins that are essential for the function of the γ -secretase complex. The Swedish mutation KM670/671NL is a double mutation in APP near the β -secretase cleavage site, which increases the production and secretion of A β [36, 37]. The arctic mutation is a single amino acid substitution, E693G, within the A β protein, which results in an increased propensity for aggregation into large soluble protofibrils [38]. The Iberian mutation, I716F, is located close to the C-terminal of A β and alters γ -secretase cleavage increasing the A β 42/40 ratio, leading to increased A β aggregation [39].

Tau

The protein tau is primarily expressed in neurons, where it stabilises microtubules [40]. Alternative splicing of the *MAPT* gene gives rise to 6 different tau isoforms in the brain [41]. Tau is a soluble protein with a natively unstructured and is generally not prone to aggregation. Still, aggregates of hyperphosphorylated tau are found in NFTs in AD brains. The exact mechanism leading to tau aggregation remains elusive, but pathological conformation changes in tau monomers and hyperphosphorylation promote aggregation and nucleation units, increasing the aggregation [42]. NFTs first appear in the transentorhinal cortex and then spread to the hippocampus, followed by extensive cortical spreading [43]. In AD, tau deposition and spreading correlate better than A β with cognitive decline and neurodegeneration [44, 45]. However, evidence points to A β as the initiator of the pathological processes that ultimately lead to AD. Temporally, A β deposition starts before tau [46], and A β oligomers enhance tau seeding [47], ultimately leading to synaptic dysfunction and tau mediated neurotoxicity. The exact mechanism behind A β and tau interplay is not known but likely important [48]. There are no known tau mutations causing AD.

Barriers of the brain

The brain parenchyma is enclosed by two distinct barriers, the BBB and blood-cerebrospinal fluid barrier (BCSFB) (Figure 3). Compared with the fenestrated and "leaky" peripheral vasculature, the brain vasculature is composed of specialised endothelial cells forming a barrier that separates the brain parenchyma from the blood circulation.

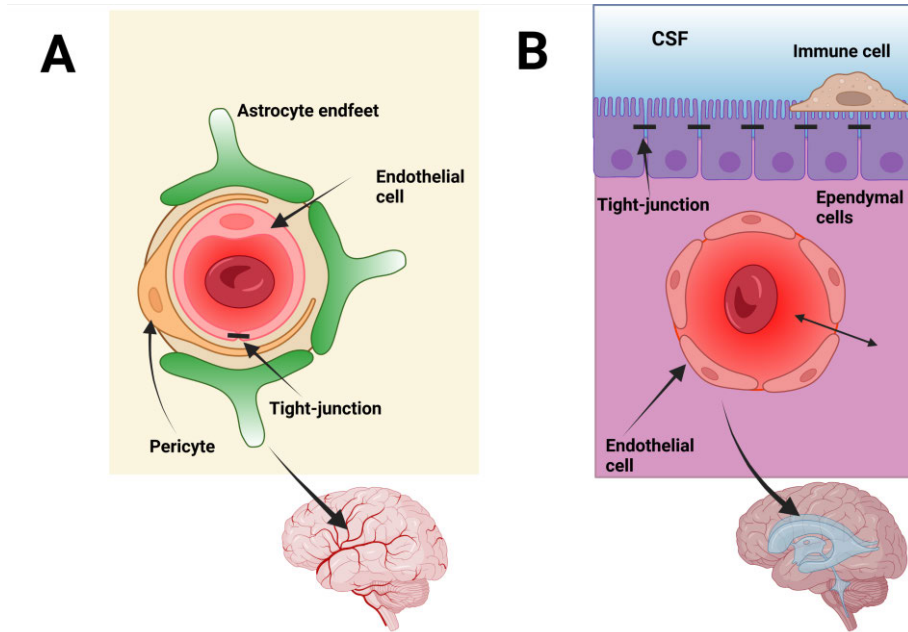


Figure 3. Illustration of the components forming (A) the blood-brain barrier (BBB), including astrocyte endfeet, pericytes, and endothelial cells connected with tight-junctions, and (B) the blood-cerebrospinal fluid barrier (BCSFB), including endothelial cells forming fenestrated capillaries, and ependymal cells connected with tight-junctions and patrolling immune cells.

BBB

The BBB is composed of tight-junction connected endothelial cells, pericytes, astrocytic endfeet projections, and neurons that together form the neurovascular unit [49]. This structure protects the brain from potentially harmful blood-borne molecules, supports the regulation of brain homeostasis, and establishes an environment viable for neurotransmission. Tight junctions are located close to the apical membrane of endothelial cells and are the main component restricting paracellular transport in between endothelial cells [50]. In addition to tight junctions, both pericytes [51] and astrocytes [52] support the BBB and contribute to the junction integrity of the barrier. A proteoglycan and glycoprotein rich viscous layer called the glycocalyx lines the luminal side of the endothelium, forming a mechanical barrier [53]. In addition, the high concentration of sugar-rich proteoglycans gives the glycocalyx a negative charge. The glycocalyx plays an important role in BBB regulation and insults to the structure result in increased BBB permeability, coagulation activation, and initiation of neuroinflammatory processes [53]. At the abluminal side of BBB, lies the basement membrane surrounding endothelial cells and pericytes [54].

At the NVU, the basement membrane provides structural support, cell anchorage and is involved in signal transduction [54]. In AD, vascular A β deposition has several detrimental effects on the NVU and the BBB, including activation of pro-inflammatory events, which could lead to increased permeability. Furthermore, A β has been reported to disrupt tight-junctions, either by altering expression of tight-junction proteins or by generating reactive oxygen species damaging tight-junctions, resulting in loss of BBB integrity [55]. In addition to structural damage, A β lowers the expression of ABCB1 protein involved in A β efflux [56].

BCSFB

The BCSFB, located at the choroid plexus in brain ventricles, is the main producer of cerebrospinal fluid (CSF), and separates the CSF and systemic circulation compartments. Unlike the BBB, the vasculature in BCSFB is permeable. Instead, tight junction between epithelial cells lining the choroid plexus establish the barrier [57]. Contrary to the BBB, the BCSFB is not an immune-privileged brain structure [58]. A variety of immune cells monitor passage of blood-derived compounds over BCSFB into the CSF.

BBB transport

Nonetheless, the brain is a highly metabolically active organ demanding a constant influx of nutrients from the circulation, which need to pass the BBB. Examples of transport routes over the BBB (Figure 4) include diapedesis of peripheral immune cells that can enter the brain under specific pathological processes in the CNS. Blood gases and small lipophilic molecules can pass the BBB and enter the brain via passive diffusion. Nutrients, such as glucose and amino acids are transported with solute carriers across the BBB. Paracellular transport (although restricted due to tight junction). Large macromolecules, such as peptides and proteins, are transported over the BBB by receptor-mediated transcytosis or adsorptive-mediated transcytosis. Brain capillaries express multiple receptors reported to facilitate brain delivery of protein ligands via receptor-mediated transcytosis (Table 1).

Table 1. Receptor-mediated transport systems located at the BBB

Receptor	Ligand
Insulin receptor	Insulin
Insulin-like growth factor receptor	Insulin-like growth factor
Low-density lipoprotein receptor	Low-density lipoprotein
Leptin receptor	Leptin
TNF α receptor	TNF α
Transferrin receptor	Transferrin

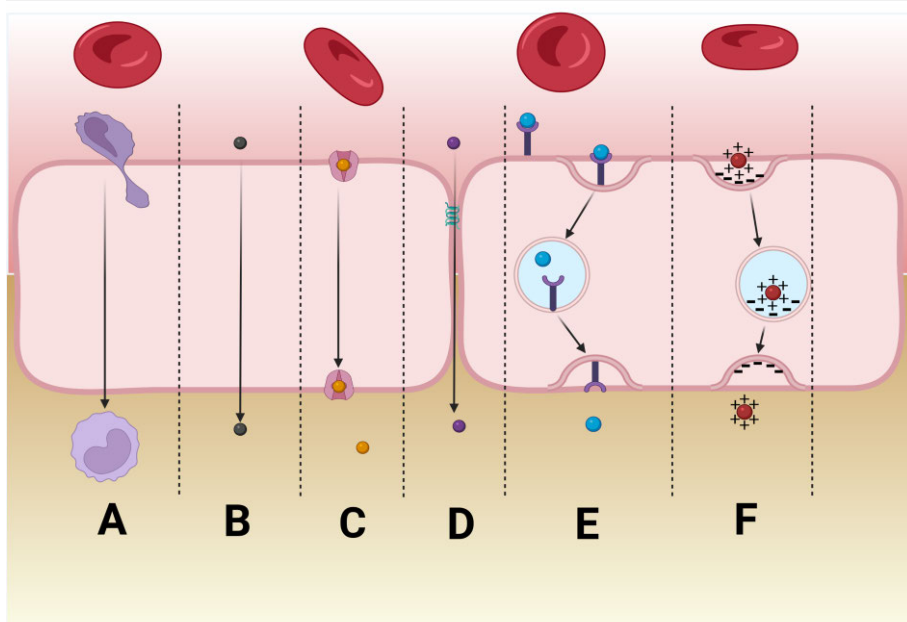


Figure 4. Transport over BBB. (A) diapedesis, (B) passive diffusion, (C) carrier-mediated transport, (D) paracellular transport, (E) receptor-mediated transcytosis, and (F) adsorptive transcytosis.

Human transferrin protein (Tf) is a 76 kDa glycoprotein produced in the liver that binds and transports iron in the blood [59]. The transferrin protein consists of near-identical lobes at the N- and C-termini, connected with a linker region [60]. Binding of ferric iron (Fe^{3+}) to transferrin is pH dependent, such that iron affinity is highest at neutral pH and affinity decreases with lowering of pH [61]. Tf can bind two iron ions, one at each lobe. A fully occupied Tf protein is called holo-Tf, whereas Tf devoid of iron is called apo-Tf [61].

Circulating holo-Tf enters cells by binding to the transferrin receptor (TfR) located at the cell membrane, which initiates clathrin-mediated endocytosis [62]. The TfR has two isoforms, TfR1 and TfR2, where TfR1 is ubiquitously expressed but especially highly expressed on rapid proliferating cells. TfR2, on the other hand, is expressed on hepatocytes, enterocytes and erythroid cells. There is a species-dependent differential gene expression of TfR, such that isolated brain microvessels from mice displayed a higher relative gene expression of the gene coding for TfR1 compared with human brain microvessels [63]. The human TfR1 receptor is a homodimer of two identical 90 kDa subunits linked with disulphite bonds. Each subunit can bind one holo-Tf protein, and TfR1-holo-Tf affinity is highest at physiological pH [64]. Brain uptake of iron is governed by TfR1 on the luminal side of endothelial cells of the BBB. The exact mechanism how iron is transported over the BBB is under debate,

and there are two main hypotheses. According to the first hypothesis, holo-Tf binding to cell surface TfR1 triggers endocytosis and formation of an endosome. Subsequent lowering of endosomal pH reduces Tf affinity to iron, which is released and pumped out of the endosome. Next, free intracellular iron is transported out of the endothelial cell and released into the brain parenchyma. The second hypothesis states that holo-Tf binding to cell surface TfR1 triggers endocytosis, but iron never dissociates from Tf, and the holo-Tf complex is transported through the endothelial cells and released into the brain parenchyma, either as free iron or holo-Tf. Shortcomings of the latter hypothesis are that more iron than Tf is transported into the brain and that it fails to explain how endothelial cells acquire iron [65].

Neuroinflammation

Neuroinflammation is an inflammatory response localised to the CNS due to trauma, infection, toxins, and hypoxia and is mediated by activated glial cells, also known as reactive gliosis. Activated glial cells release signal molecules, including pro-inflammatory cytokines, chemokines, and reactive oxygen species [66]. Short term or acute neuroinflammation can be beneficial if inflammation can be resolved. On the other hand, chronic inflammation has an apparent detrimental effect on the brain, causing a self-perpetuating cycle, and in the context of AD this contributes to disease progression. Studies with PET tracers for neuroinflammatory imaging have hinted at a bi-phasic activation pattern [67], indicating an initial attempt to clear and resolve the inflammation, but ultimately fails giving rise to chronic neuroinflammation seen in AD [68].

Astrocytes

Astrocytes are star-shaped glial cells with a neuronal origin, and support brain homeostasis in multiple ways, including, contribution to the BBB, fluid maintenance, neuronal synaptic activity and remodelling, neurotransmitter metabolism [69], and as a vital player in the brain's glymphatic system [[70]. In the context of AD, reactive astrocytes close to A β plaques change morphology and develop hypertrophic processes and increased expression of glial fibrillary acidic protein (GFAP). Astrocytes have been reported to be involved in A β clearance [33] and *post-mortem* studies of AD brains reveal astrocytes containing amyloid granules close to plaques hinting at attempted A β clearance [71].

Microglia

Microglia have a myeloid origin and are considered the brain's professional phagocytic cells. In the brain, microglia survey the environment and maintain tissue homeostasis. They are also important in neuronal development, regulating neuronal apoptosis, synaptic pruning, and synaptic plasticity [72]. As with

astrocytes, if microglia sense pathological stimuli they become activated, releasing inflammatory mediators. Microglia close to plaques display intracellular A β deposits, suggesting they are engaged in plaque removal [73].

The triggering receptor expressed on myeloid cells 2 (TREM2) has surfaced as a potential biomarker for AD progression in recent years. TREM2 is expressed on the microglial cell membrane and consists of an extracellular, a transmembrane and an intracellular domain. TREM2's extracellular domain can be cleaved off, generating soluble TREM2 (sTREM2) [74]. TREM2 is an active player in innate immune responses and binding of lipids, lipoproteins, apolipoproteins, including apolipoprotein E, initiating downstream signalling pathways that modulate proliferation, phagocytosis and inflammation [75, 76]. Identification of several AD-associated TREM2 mutations has revealed plausible ways how TREM2 is involved in pathological processes in AD, such as microglial clustering at A β plaques [77].

Diagnostic biomarkers in AD

Biomarkers can be defined as cellular, biochemical, or molecular constituents that can be measured in biological materials such as fluids, cells or tissues and reflect biological processes or pathological changes [78].

Fluid biomarkers

Compared with many peripheral tissues, brain tissue is inaccessible for direct measurement by biopsy sampling. Nonetheless, CSF sampling and brain imaging can be utilised to illuminate processes that reflect brain function. CSF is a transparent fluid produced by the choroid plexus of the brain ventricles. Pulsations drive the CSF flow from the ventricular system into the brain and spinal cord's subarachnoid space and the CSF is ultimately reabsorbed by several routes, including blood absorption via venous sinuses of the arachnoid villi or lymphatic absorbance [79].

In the context of AD, CSF measurements of A β , total tau (T-tau) and phosphorylated tau (P-tau) are all used in the diagnosis of AD. Alterations in these markers are already seen at an early stage of AD [80], where patients typically show low CSF concentration of A β 42. This is likely because of sequestration of A β 42 in plaques, and thus, A β 42 levels in CSF correlate inversely with brain levels [81]. A β 40 is more abundant in CSF, but remains stable and does not correlate with brain levels, and is thus not in itself used as a marker in AD. However, measuring the A β 42/A β 40 ratio in CSF provides a better predictive indication of risk for AD progression than CSF A β 42 levels alone [82, 83]. T-tau and P-tau concentrations are both elevated in CSF in AD patients. An increase in CSF T-tau indicates neuronal death and axonal damage, whereas high CSF P-tau indicates the presence of NFTs in the AD brain [84, 85].

As aberrant microglia activation is seen in AD, measuring released protein components of the neuroinflammatory processes could aid in understanding the disease progress and be used as a diagnostic marker. Due to microglia's central position acting as a key player in neuroinflammation, intensive research has tried to identify biomarkers in microglial activation. One interesting biomarker for microglial activation is TREM2. Increased levels of sTREM2 have been found in CSF and correlate with high CSF T-tau and P-tau [86].

Compared with CSF sampling and brain imaging, blood sampling is less invasive, less expensive, and is routinely performed at all levels of the healthcare system. The discovery of blood biomarkers related to AD could be of great use in population screening and as a tool for the early identification of individuals that could benefit from therapeutic intervention. As a result of receptor mediated transport and CSF drainage of AD related proteins into the blood, brain derived biomarkers can be measured in the systemic circulation. Initial ELISA-based measurements of plasma A β 42/A β 40 were inconclusive in determining a difference between AD patients and controls [87]. More recently, it was reported that using a single-molecule array (SIMO) assay, a weak but significant correlation of plasma and CSF levels of A β 42 and A β 40 and an inverse correlation between amyloid PET and plasma A β 42 was found in the Swedish BioFINDER cohort [88]. Combining immunoprecipitation and mass spectrometry for quantifying plasma APP/A β 42 and A β 40/A β 42 ratios brain A β could be predicted with 90% accuracy [89]. Although promising, quantification of plasma A β is confounded by A β production in peripheral tissues [90]. Plasma P-tau has sprung up as a biomarker useful for discrimination of AD from non-AD. Plasma P-tau181 is increased and followed AD progression and correlated with positive tau PET [91], and discriminate AD from non-AD 8 years before death [92]. Recently, plasma P-tau217 has risen as marker with better discriminative accuracy than P-tau181 in differentiating AD from non-AD [93].

PET imaging in AD

Amyloid PET can help clinicians in the diagnosis of AD and be used for inclusion of patients or as a tool to measure therapeutic effects in clinical trials. PET has also been extensively used in research to understand the disease process. [^{11}C]Pittsburgh compound B ([^{11}C]PiB) is a derivate of thioflavin-T and was the first PET tracer for imaging amyloid deposits in AD patients [94]. PiB binds with high affinity to the β -sheet structure of insoluble amyloid fibrils [95], and with low affinity to protein aggregates in NFT and Lewy bodies. A shortcoming of [^{11}C]PiB PET, and all ^{11}C labelled tracers, is the half-life of ^{11}C (20 min) that requires on-site cyclotron production of the radionuclide. Development of ^{18}F ($T_{1/2}$ 110min) labelled amyloid PET tracers have increased

availability and regional delivery. Second generation ^{18}F labelled tracers, approved by the FDA, are [^{18}F]florbetapir, [^{18}F]florbetaben, and [^{18}F]flutemetamol [96]. A drawback shared by [^{11}C]PiB and other amyloid PET tracers based on small drug-like compounds is that they only reflect the burden of insoluble A β plaques and not the toxic soluble and diffuse A β aggregates. Since the amyloid burden reaches a plateau early in the disease progression, [^{11}C]PiB PET signal remains stable and fails to detect disease progression at later stages [97]. However, amyloid PET can be used to identify AD patients at an early stage in the disease development [98].

Accumulation of hyperphosphorylated tau is seen in multiple neurodegenerative diseases, including AD. Not unexpectedly, multiple tau PET tracers have been developed for quantification of tau deposition in the brain. A first generation tau tracer, [^{18}F]THK523, displayed specific tau binding, and tau transgenic mice, compared to wild-type (WT) mice, displayed increased tracer retention [99]. Furthermore, [^{18}F]THK523 brain uptake was elevated in AD patients, but high monoamine oxidase-B (MAO-B) [100] and white matter binding complicated quantification of PET images in a clinical setting [101]. A second generation tau tracer, [^{18}F]flortaucipir (AV-1451 or T807), has been approved by the FDA to image tau pathology in AD. Assessment of flortaucipir's binding properties in *in vitro* studies on *post-mortem* brain tissues from AD patients have demonstrated that flortaucipir binds with high affinity to NFTs [102, 103]. Subsequent clinical studies have demonstrated the usability of [^{18}F]flortaucipir PET, in which tracer retention follows brain tau distribution and correlates with AD symptomatology [45, 104]. However, [^{18}F]flortaucipir PET shows off-target binding, to MAO proteins [105] and substantia nigra [106, 107].

The involvement of astrocytes and microglia in AD has prompted the development of PET tracers to investigate neuroinflammatory processes in the AD brain. The 18 kDa translocator protein (TSPO) is the most well-studied neuroinflammatory PET target. TSPO is expressed in the mitochondrial membrane of astrocytes and microglia, and expression is upregulated in neuroinflammation [108]. A first-generation TSPO PET ligand, [^{11}C]PK-11195, has been extensively evaluated for neuroinflammation imaging in AD, and a positive correlation between [^{11}C]PK-11195 and [^{11}C]PiB retention occurs in brains of patients with mild cognitive impairment [109]. Yet, a drawback with [^{11}C]PK-11195 is high background due to low BBB penetration and binding to plasma proteins [110]. Development of second and third generations of TSPO ligands have overcome some of the limitations mentioned above with PK-11195. Still, these new TSPO ligands suffer from large interindividual variation in TSPO binding due to the genetic polymorphism rs6971 in the TSPO gene [111].

Immunotherapy in Alzheimer's disease

With the realisation that A β plays a central role in AD, it has been hypothesised that reducing A β production or enhancing its brain clearance could halt disease progression. For a long time, the future of immunotherapy in AD seemed bleak after multiple anti-A β antibodies failed in clinical trials. Factors contributing to this are targeting of wrong A β species or suboptimal patient selection. The recent FDA approval of *aducanumab* has invigorated and highlighted the feasibility of brain directed immunotherapy in AD.

Active immunisation

Active immunisation, or vaccination with A β , has been evaluated as a therapeutic approach in AD. An initial study in an AD mouse model demonstrated that vaccination with full length synthetic A β ₄₂ lowered brain A β and improved cognitive function in behavioural tests [112]. In a clinical phase IIb trial with synthetic A β ₄₂ (AN-1792) given to patients with mild to moderate AD, only 19.7% developed an antibody response, and the study was terminated due to meningoencephalitis in 6% of participants [113]. A T-cell epitope in the mid region of A β is believed to cause an A β -specific T-cell response leading to meningoencephalitis seen in vaccination with full length A β [114]. To circumvent unfavourable T-cell activation, subsequent immunisation trials have utilised N-terminal fragments of A β , lacking T-cell epitopes [115]. Compared with AN-1792, none of the clinical trials with second generation A β vaccines have so far resulted in meningoencephalitis, demonstrating their safety. Although safe, no second generation vaccines have shown any clinical benefits, but several vaccines are still being evaluated in phase II studies [116]. An alternative approach in active immunisation involves stabilising specific aggregation forms of A β by introducing intramolecular disulfate bonds in A β monomers. The resulting A β molecule adopts a stable beta-hairpin structure prompting the formation of A β oligomers, but without further fibrillisation [117]. In October 2021, a phase 1b study launched where early AD patients received active vaccination with A β stabilised in oligomeric form [118].

Passive immunisation

In passive immunisation, an unimmunised person is administered an exogenous source of antibodies giving a temporary humoral immunity towards the antigen. The benefits of passive immunisation are that the antibody concentration can be adjusted to achieve an optimal treatment effect. This could be especially important in an ageing population that display reduced humoral response to active immunisation [119]. The identification of A β deposition as an early pathological event in AD has initiated the development of multiple anti-A β monoclonal antibodies that have been evaluated in clinical trials (Table 2). Several hypotheses have been put

forward on how antibodies can reduce brain A β . These include blocking fibrillar or oligomeric A β elongation, microglia mediated phagocytosis of A β , or enhancement of brain A β efflux through a peripheral sink effect.

Table 2. Anti-A β antibodies (and their A β epitopes), which have been or are currently evaluated in clinical trials.

Name	Aβ epitope	Status
Bapineuzumab	N-terminal (A β 1-5), no A β species selectivity [120]	Failed
Solanezumab	Mid region (A β 16-26), soluble monomeric A β [121]	Failed
Gantenerumab	N-terminal (A β 3-7), mid region (A β 18-27), preferable fibrillar A β [122]	Ongoing, phase III
Donanemab	Pyroglutamate form of A β (A β p3-42), bind A β plaques [123]	Ongoing, phase III
Aducanumab	Conformational selective, insoluble A β fibrils and A β oligomers [124]	Approved, phase IV
Lecanemab	Conformational selective, mainly A β protofibrils, also oligomeric and fibrillar A β [125]	Ongoing, phase III

Bapineuzumab

Bapineuzumab (humanised version of the mouse antibody 3D6) binds to the N-terminal end of A β and displays no selectivity among different A β species [120]. *Bapineuzumab* was the first passive immunotherapy antibody tried in AD patients and has been extensively evaluated in large phase III trials; however, compared to control, no beneficial clinical effects were seen among patients with mild to moderate AD [126]. The *bapineuzumab* trials were partially terminated due to vascular disturbances seen as amyloid-related imaging abnormalities (ARIA) [127, 128].

Aducanumab

Aducanumab (Aduhelm) is a conformation-selective monoclonal antibody recognising insoluble A β fibrils and soluble A β aggregates, but not A β monomers [124]. A first in human study involving 56 patients with mild to moderate AD demonstrated that *aducanumab* was safe in doses up to 30 mg/kg, whereas ARIA was seen in all patients receiving the highest dose, 60 mg/kg [129]. PRIME, a phase 1b follow-up study, including 165 AD patients demonstrated a dose-dependant lowering in amyloid PET and slowing of clinical progression [124]. The success of the PRIME study prompted the launch of two large phase III clinical trials, EMERGE and ENGAGE. Eligible

patients had MCI or amyloid PET-positive mild dementia. In 2019, Biogen announced that both trials were halted because of the unlikelihood that the clinical endpoints would be met [130]. However, re-analysis of EMERGE trial data showed that primary and secondary endpoints, such as slowing of clinical decline, were met in the highest dose group [131]. Not without controversy, in June 2021, the FDA issued an accelerated approval of *aducanumab* (Aduhelm) to treat AD.

Lecanemab

Large soluble A β species (oligomers and protofibrils) are believed to correlate better than insoluble A β fibrils with AD progression and seems to be more neurotoxic. Targeting them instead of fibrillar or monomeric A β with antibodies could potentially halt disease progression [132]. *Lecanemab* is the humanised version of mAb158, developed in our lab, that displays preferable binding to A β protofibrils over monomeric and fibrillar A β , and does not bind to soluble fragments of APP [133]. Preclinical studies in transgenic mice demonstrated that mAb158 injected weekly for 13 weeks significantly reduced brain protofibril levels in a dose-dependent manner [125]. These findings have prompted progression to human clinical trials, and a phase IIb trial including 856 early AD patients demonstrated lowering of brain A β in a dose-dependent manner and slowed clinical decline. *Lecanemab* was well-tolerated with <10% ARIA-E among patients receiving the highest dose [134]. The successful phase IIb trial prompted the launch of a large phase III trial. *Lecanemab* proceeded into a large phase III study in March 2019 [135].

Enhancement of antibody brain uptake

From a neuropharmacological perspective the effectiveness of BBB limits the delivery of pharmacological compounds to targets in the brain parenchyma. Nonetheless, it has been reported that approximately 0.1% of injected antibodies enter the brain [136], although this number might be an overestimation of true antibody brain uptake because CSF measurement as a proxy for brain parenchyma overestimates brain levels due to greater antibody penetration over the BCSFB [137].

Large proteins, such as antibodies, cannot efficiently penetrate the BBB. Instead, a variety of concepts have been explored to enhance brain uptake of large compounds, including invasive techniques that cause temporary BBB disturbance by pharmacological means [138] or by focused ultrasound [139-141]. A less invasive method is the utilisation of endogenous transcytosis systems such as the insulin receptor [142], insulin-like growth factor-1 [143], Tmem30a [144, 145], or the transferrin receptor [146, 147], located at the surface of endothelial cells forming the BBB. The availability of receptors that mediate receptor-mediated transcytosis (RMT) of compounds across the BBB

has promoted the development of molecular "trojan horses", which utilise endogenous RMT systems for enhanced brain uptake. An example is bispecific antibody constructs that bind to the protein mediating RMT across the BBB, with subsequent release into the brain parenchyma for interactions with the target molecule [148] (Figure 6).

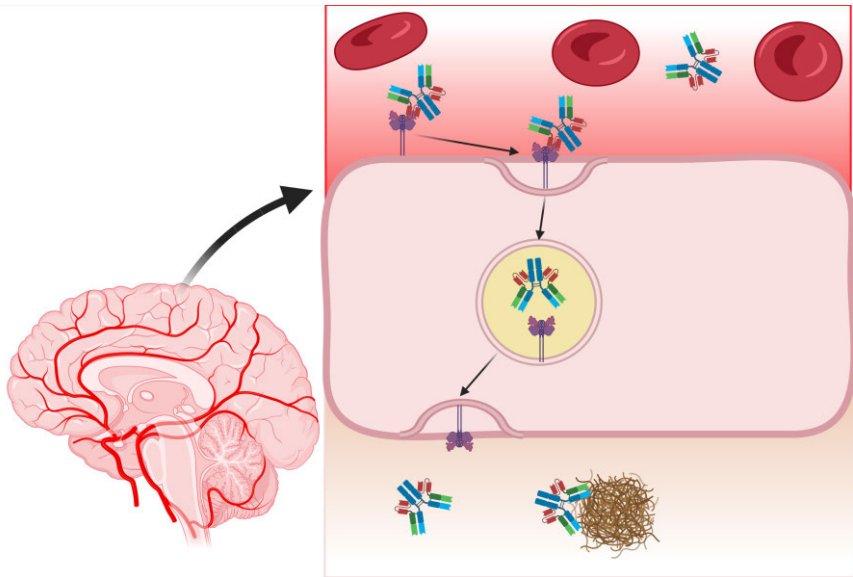


Figure 5. Presumed mechanism behind TfR brain shuttling of protein therapeutics. In this case, a bispecific antibody targeting TfR and A β binds to the extracellular domain of TfR, forming a complex. The bispecific antibody-TfR complex is internalised within a vesicle. The bispecific antibody dissociates from TfR, is transported to the abluminal side and released into the brain parenchyma where it interacts with A β .

Ideally, to be successful as an RMT bispecific antibody, specific criteria need to be fulfilled: (1) The antibody must bind to the extracellular domain of the RMT protein facing the blood vessel lumen. (2) The antibody should bind off-site of endogenous ligands so as not to interfere with the endogenous cellular processes. (3) The antibody should target the RMT system while evading the endolysosomal degradation pathway, and (4) the bispecific construct should efficiently be transported to the abluminal membrane of the endothelial cell and released into the brain parenchyma.

One of the most studied RMT systems that have been explored in brain protein therapeutics is TfR, and research has pinpointed several essential factors that need to be considered for successful brain delivery. The affinity of the antibody towards TfR is an important determinant of successful BBB transcytosis [149, 150]. Antibodies that target the TfR with moderate to low affinity show greatest BBB penetrance [151]. Also the valency of the TfR

interaction is important. Monovalent TfR binding is favourable and results in a higher degree of successful BBB transcytosis. Bivalent TfR interaction, on the other hand, seems to alter intracellular trafficking and shift transport to the lysosome for degradation. Probably due to TfR clustering [152]. In addition, administered dose also influences BBB transcytosis [153, 154].

The monoclonal antibody 8D3 is a rat anti-mouse TfR antibody that has been extensively used in antibody constructs to increase brain uptake [152, 153, 155-158]. We have created multiple A β -binding bispecific antibody constructs based on 8D3 (Figure 6) [154]. The first construct was a F(ab)₂ of the humanized mAb158 chemically linked with 8D3. When radiolabeled with iodine-124 (¹²⁴I), PET imaging with the bispecific construct could detect and quantify A β load in transgenic mice [156]. We improved the format by recombinantly expressing a single-chain variable fragment (scFv) of 8D3 linked to the C-termini of mAb158's light chains. RmAb158-scFv8D3, compared with unmodified mAb158, displayed 80-fold higher brain uptake 2 h after injection [153]. To improve PET imaging we have created two smaller bispecific versions. The first version is a 100 kDa bispecific TribodyTM construct containing two mAb158 scFv connected to a Fab fragment of 8D3 [157]. The second construct is a tandem di-scFv of 3D6 and 8D3 [155]. The 58 kDa tandem di-scFv construct lies just at the renal clearance threshold and is rapidly cleared from the blood.

Brain elimination of therapeutic antibodies

Inside the brain, there are multiple pathways a therapeutic antibody bound to its target can be eliminated through. The formation of antigen-antibody immunocomplexes in the brain can also trigger phagocytic degradation processes. Microglia fulfill this role as the professional phagocytic cell in the brain. Microglia cells express cell surface Fc γ -receptors (Fc γ R) that bind to the antigen-antibody complex, triggering engulfment and phagocytosis of immunocomplexes [159]. The glymphatic system could also be implicated in clearance of antigen-antibody complexes. The glymphatic system depends on convective flow generated by aquaporin 4 channels located at astrocytic end-feet projections. The convective flow in brain parenchyma transports solutes, in this case immuno complexes, toward perivenous spaces where it is collected. Lastly, the fluid in perivenous space drains into the cervical lymphatic system [70]. The role of the aquaporin 4-generated contribution to convective flow has come into question due to the high hydrostatic resistance in the brain parenchyma, which favors diffusion transport [160].

ImmunoPET imaging with bispecific antibodies

ImmunoPET is based on radiolabelling of an antibody with a positron-emitting radionuclide. There are several advantages of immunoPET. For example, antibodies can be created to target a variety of antigens, including specific post-translation modification or aggregation states of proteins. Another attractive property of immunoPET is theranostic imaging. The imaging (diagnostic) target is the same as the therapy target. Compared with PiB, which binds insoluble fibrils found at the core of plaques, antibodies can bind to A β aggregates in the diffuse halo surrounding the plaque core. With immunoPET, bispecific antibodies can image soluble A β burden *in vivo*. We have demonstrated that radiolabeled RmAb158-scFv8D3 can be used as a PET tracer if labeled with ^{124}I or ^{18}F . In a transgenic AD mouse model, PET imaging of RmAb158-scFv8D3 permitted A β to be visualized 72 h after injection. Tracer retention closely correlated to pathological burden [153] and detected changes in A β burden after A β lowering treatments [161, 162]. The half-life in blood of a compound directly translates to its usability as a PET-tracer. Ideally, to achieve a high contrast image, the radiolabelled compound should bind to its target with high affinity and display fast blood clearance because prolonged blood retention will give rise to high signal background. Due to its size of 58 kDa, our di-scFv construct has a blood half-life of 3-4 h, which enables earlier PET imaging (~24h after injection) compared with the full-size bispecific antibody [155].

Anti-drug antibodies

The introduction of biological therapeutics for the treatment of disease has presented new challenges in which the host immune system can initiate immunological responses because the biotherapeutic drug is recognised as foreign by the body. One outcome can be an induction of humoral responses, including anti-drug antibodies (ADA), that target the protein drugs. ADA may lead to loss of drug effectiveness or side effects and may even be life-threatening [163]. As such, regulatory agencies require ADA responses to be monitored during trials with biological therapeutics. Although a serious issue, the shift toward humanised or fully human antibodies in immunotherapy has largely mitigated the problem with ADA in humans. ADAs against protein drugs are classified as neutralising (NAb) or non-neutralising (non-NAb) antibodies, both of which reduce efficacy through different mechanisms. NAb blocks a drug's pharmacological function by binding to and sterically preventing target binding, whereas non-NAb binds to the drug and enhances clearance [164]. Protein drugs forming large *in vivo* aggregates can cross-link B-cell receptors and initiate ADA production, leading to an early release of IgM antibodies that bind to the protein drug [165].

Protein drug aggregates can also incite uptake by splenic residing B-cells, which digest the protein to a 12-15 amino acid peptide sequence that are loaded and presented by the B cell MHC II receptor [166, 167]. If the MHCII-peptide complex is recognised by CD4⁺ T helper cells (T_H cells), primed B-cells migrate to lymph nodes and interact with follicular T_H cells, which in turn migrate to the follicular germinal center, activating B-cells to form antibody-producing plasma cells. Repeated immunogenic stimulus causes Ig class switching and affinity maturation, producing high-affinity binding ADA [167].

Aim

This thesis aimed to improve AD treatment and diagnostics by evaluating and comparing a bispecific brain penetrating anti-A β antibody, RmAb158-scFv8D3, to its parent version, RmAb158. We assessed brain uptake and intra-brain distribution of both antibodies with different types of radiolabeling. We also evaluated treatment efficacy in A β mouse models and studied whether BBB permeability to large molecules is affected following acute treatment with an anti-A β antibody.

Paper I

To investigate BBB permeability to large molecules in tg-ArcSwe mice and age-matched WT mice, with or without single dose anti-A β antibody treatment.

Paper II

To compare long-term brain uptake, spatial distribution, and blood pharmacokinetics of the monospecific A β targeting antibody, RmAb158, with its bispecific variant, RmAb158-scFv8D3, in 18 months old tg-ArcSwe mice.

Paper III

To explore how ^{111}In labelling with compatible chelators affect brain uptake and peripheral biodistribution of RmAb158-scFv8D3 in 18 month old tg-ArcSwe and age-matched WT mice.

Paper IV

To evaluate the therapeutic effects of RmAb158-scFv8D3 in comparison with RmAb158 in a multi-treatment study design in *App*^{NL-G-F} mice. Furthermore, we assessed the immunogenicity of RmAb158-scFv8D3 and attempted to design an immune evading variant.

Methods

Animal models

Animal models have become an invaluable tool in modern biological or medical research, providing researchers with a way to address and investigate normal biology and pathological processes in a complex biological system. The most commonly used animals are mice and rats, accounting for the majority of all laboratory animals used. The use of mice is frequent in AD research, in which several transgenic and gene knock-in mouse lines have been created recapitulating different pathological aspects of AD.

Tg-ArcSwe

Tg-ArcSwe is a transgenic mouse model expressing the human *APP* gene (isoform 695) with the Swedish (KM670/671NL) and Arctic (E693G) mutations, which increase A β production and promote aggregation, respectively. The gene is expressed under the neuron-specific Thy1 promoter and the model exhibits a three-fold overexpression of human APP. Intracellular A β starts to accumulate from 1 month of age followed by parenchymal plaque formation from 5-6 months of age. Brain levels of A β protofibrils and total A β increase with age and in older transgenic mice there is a larger interindividual difference in A β burden, a problem that most A β mouse models have. A β deposition is found in the cortex, hippocampus and thalamus, and at later stages also in the cerebellum [168, 169]. The plaque morphology in Tg-ArcSwe mice resembles that seen in AD patients, with dense core A β plaques [169]. Vessel-associated A β pathology (CAA) is also abundant in thalamic and cortical blood vessels [169]. Tg-ArcSwe mice exhibit spatial learning deficit inversely proportional to A β protofibril concentration [170].

App^{NL-G-F}

App^{NL-G-F} is a human *APP* gene knock-in mouse model containing the Swedish (KM670/671NL), Arctic (E693G) and Iberian (I716F) mutations. Like the Tg-ArcSwe model, the Swedish and Arctic mutations increase A β production and promote A β aggregation. The addition of the Iberian mutation, I716F, affects γ -secretase cleavage and increases the A β 42/A β 40 ratio. Homozygous *App*^{NL-G-F} mice present with early cortical A β deposition, starting from 2 months of age and deposition increases with age. Subcortical A β deposition starts from

4 months of age and increases with age. The mouse model also displays pronounced neuroinflammatory alterations with astro- and microgliosis surrounding A β plaques. Lastly, *App*^{NL-G-F} mice present with synaptic changes, a decrease in synaptophysin and PSD95 staining near A β plaques, and memory impairment [39].

Recombinant expression of bispecific antibodies

Antibodies used in the present studies were in-house produced according to Fang et al. [171]. The construct sequence was cloned into a pcDNA3.4 vector and transfected into *E.coli* (TOP 10 cells). Bacteria were expanded and plasmid DNA was extracted. Expi293 cells were used as the expression system. The cells were transfected with plasmid DNA and incubated for 7 days. Constructs were isolated from cell medium with affinity chromatography. Full-size antibodies were isolated with a protein G column (which binds to the Fc or Fab region) and eluted by pH change. Constructs lacking Fc regions, but congaing a His-tag, were isolated using a nickel-ion column (binding to the His-tag) and eluted with imidazole. Buffer exchange was performed to transfer produced antibodies (Figure 6) in a suitable buffer for subsequent experiments.

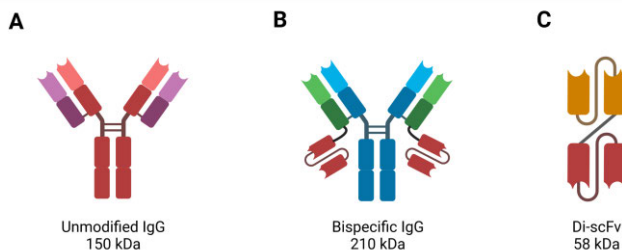


Figure 6. Produced antibodies/antibody constructs. (A) unmodified IgG. In **paper I**, 3D6; **paper II** and **IV**, RmAb158. (B) In **paper II-IV**, bispecific antibody (IgG) based on RmAb158 and scFv fragments of mTfR binding antibody 8D3. (C) **paper IV**, di-scFv of 3D6 and 8D3 antibodies (di-scFv3D6-8D3).

Design of antibodies with reduced immunogenicity

Since 8D3 is a rat-derived antibody and since our bispecific proteins contain various linkers between protein domains, we attempted to lower their immunogenicity in mice by selectively mutating the protein to lower a potential ADA response toward RmAb158-scFv8D3.

Phagocytosis of foreign peptides with subsequent proteolytic fragmentation and MHCII presentation of peptide fragments is a major step in initiating CD⁴⁺

T-cell mediated humoral response. In **paper IV**, scFv8D3 (rat-derived antibody fragment) and the linker connecting it to RmAb158-scFv8D3 were subjected to *in silico* analysis of potential MHCII binding affinity, using the MHCII binding prediction tool (<http://tools.immuneepitope.org/mhcii/>) at the **Immune Epitope Database (IEDB)** analysis resource. Sequences predicted to bind with high affinity to the MHC II receptor were selected for amino acid substitution. To decrease the risk of reducing mTfR binding of scFv8D3, amino acid substitutions in the CDR regions were kept to a minimum. In addition, proline and cysteine residues were not altered due to the risk of causing alterations in protein secondary structure and formation of new intra-peptide disulfide bonds, respectively. Non-restricted amino acids were systematically changed and re-analysed in the MCH II binding predictor until a maximum reduction in MHC II binding was attained.

Radioiodine labelling of antibodies

Antibodies used in the projects were labelled with iodine radioisotopes to investigate tissue uptake and biodistribution of administered radioactive compounds. Macromolecules such as proteins can readily be directly radioiodinated using an oxidising agent such as chloramine-T. Oxidation of radioiodine results in an electropositive form, which subsequently can form an iodine-carbone bond of predominantly tyrosine residues. The two main iodine radioisotopes used in this work were ^{125}I and ^{124}I . ^{125}I has a half-life of 60 days and decays via electron capture, emitting with maximum energy of 35 keV photons and electrons (auger and conversion electrons) and its main use is in biological assays. ^{124}I has a half-life of 4.2 days and decays 74.4% via electron capture and 25.6% via positron emission (mean energy: 819 keV), and thus, can be used in PET. In **papers I, II, and IV**, antibodies were directly labelled using chloramine T. Reactions were quenched with the reducing agent sodium metabisulfite, and radiolabelled antibodies were purified with size exclusion chromatography. In **papers I, II, and IV**, antibodies were labelled with ^{125}I to facilitate investigation of blood pharmacokinetics, tissue retention, spatial brain distribution and to enable longitudinal SPECT imaging (**paper II**). In **paper IV**, RmAb158-scFv8D3 was labelled with ^{124}I to facilitate dynamic PET imaging of biodistribution in immunised mice. Since chloramine T is an oxidising agent that can disrupt intra protein bonds and severely damage the ability of antibodies to bind their antigen, all iodinate antibodies underwent a post-labelling binding assay with ELISA.

Radiometal labelling of antibodies

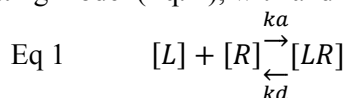
Since metals do not readily form a covalent bond to carbon atoms, an alternative approach is needed to attach radiometals to proteins. Proteins are func-

tionalised by conjugating a bifunctional chelator that facilitates radiometal labelling through the chelate effect, where one or more functional groups (such as O, N, and S) of the chelator molecule donate electrons facilitating metal binding. Successful labelling depends on properties of the radiometal ion, such as ion charge and radius, and the match of chelator. For successful labelling, the size of the chelator's binding pocket needs to accommodate the radiometal and coordination number should match the radiometal's ionic charge and adopt a suitable coordination geometry.

In **paper III**, RmAb158-scFv8D3 was labeled with ^{111}In . The radiometal ^{111}In has a half-life of 2.8 days and decays via electron capture, emitting 171 keV (90%) and 245 keV (94%) γ -rays. The relative low γ -ray energy, high percentage of detectable γ -rays together with a 2.8 days half-life makes ^{111}In a good radionuclide for use in antibody-based SPECT imaging. To facilitate ^{111}In labelling, RmAb158-scFv8D3 was functionalised with either CHX-A''-DTPA, DOTA, or by a multistep process involving *in vitro* inverse electron demand Diels-Alder (IEDDA) reaction. In the first step, RmAb158-scFv8D3 is conjugated with transcyclooctene (TCO). Subsequently, tetrazine-DOTA was labelled with ^{111}In and [^{111}In]tetrazine-DOTA was clicked with TCO-RmAb158-scFv8D3.

Real-time measurement of tracer kinetics using LigandTracer

LigandTracer is a technique for real-time measurement of ligand-receptor interactions, either as protein-protein or protein-cell interactions. The assay is based on a tilted rotating support with a fluorescent or γ -ray detector. Cells or proteins are coated on a cell culturing dish in a defined target area and placed on the rotating support. Ligand solution is added, and the support slowly rotates, taking multiple measurements from the target area and a defined reference area. The association phase of ligand-receptor formation is evaluated with two or more different ligand concentrations, followed by a dissociation phase. In **paper II**, the kinetic parameters, k_a , and k_d , and binding affinity, K_D , were evaluated with LigandTracer. [^{125}I]RmAb158 and [^{125}I]RmAb158-scFv8D3 binding to A β protofibrils and [^{125}I]RmAb158-scFv8D3 binding to mTfR were analysed and kinetic parameters were extracted with a 1:1 curve fitting model (Eq. 1), with and without correction for depletion of the ligand.



Molecular imaging

Molecular imaging includes imaging techniques that permit investigation of biological processes *in vivo*, and provides means of studying molecular processes in health and disease in the natural context inside a living organism. PET and SPECT are examples of molecular imaging techniques in which high-energy photons can be detected and quantified *in vivo*. Of importance is the choice of radionuclide, in which the physical half-life of the decaying isotope needs to be long enough to encompass distribution, target binding, and blood elimination of radiolabelled compound. Additional desired properties include a decay mode with high percentage of low energy positron emission (PET) and γ -ray emission with energy of 100-200 keV (SPECT). In **paper II-IV**, RmAb158 and RmAb158-scFv8D3 were radiolabelled with ^{125}I , ^{124}I , or ^{111}In , and mice were scanned earliest three days after injection to achieve optimal imaging contrast [154], i.e. high target binding and low blood-derived background signal.

PET

PET relies on coincident detection of the annihilation event when a positron (β^+) combines with an electron, and in the process emits two 511 keV photons traveling in opposing direction (180°) [172]. A detector ring registers the annihilation photons, and only near instant (<10 ns) detection of two photons constitutes a true detection event. The location of the annihilation event is estimated by the line-of-response between the two detectors that record the annihilation photons [173]. In **paper IV**, dynamic PET, 0-60 min, was used to investigate how biodistribution differed between naïve and immunised mice, after treatment with mutated RmAb158-scFv8D3. From the point of [^{124}I]RmAb158-svFv8D3^{mut} injection, the acquisition was recorded in event-by-event mode (list mode) to enable dynamic PET. Data were reconstructed in several time frames, in which changing radioactivity retention was investigated.

SPECT

In SPECT, a single photon is detected from the decay of γ -emitting radionuclides. By rotating detector head(s) around the subject, a volume of radioactivity will be collected. SPECT incorporates collimators that only allow passage of γ rays of a specific angle so that the point of origin of activity distribution can be determined [174]. A drawback with the collimator is a reduced sensitivity because most γ rays are blocked [175]. In **paper II**, radiolabelling RmAb158 and RmAb158-scFv8D3 with ^{125}I ($t_{1/2}$ 59.5 days) enabled SPECT imaging of brain retention of radioiodinated antibodies over a month. In **paper III**, RmAb158-scFv8D3 was conjugated with CHX-A''-DTPA or DOTA to facilitate labelling with ^{111}In (SPECT radionuclide). Whole-body distribution and tissue retention of ^{111}In labelled RmAb158-scFv8D3 was investigated

three days after injection in 18 month old tg-ArcSwe and aged-matched WT mice. In **paper IV**, SPECT was used to visualise the depletion of CD4⁺ T-cells following immunodepletion with an anti-CD4 antibody.

Assessment of BBB permeability

Multiple lines of evidence indicate that the integrity of the BBB is affected in AD. The likely culprit is vascular A β deposits or CAA, destabilising the BBB and increasing permeability, probably mediated by inflammation. Further exaggerating permeability is anti-A β antibodies binding to CAA. Dextran is a polymer of sugar molecules not actively transported over the BBB, making them a good tool for assessing BBB permeability.

In **paper I** we investigated whether BBB permeability is increased in tg-ArcSwe with or without a single dose of 3D6. Permeability was assessed with two different sized dextran molecules, a 4 kDa fluorescein-labelled dextran and a 150 kDa Antonia red-labelled dextran. Aged tg-ArcSwe and WT mice were i.v. injected with [¹²⁵I]3D6 or PBS as control, and the treatment period was 72 h. Mice received both dextrans by i.v. injection just before intracardiac perfusion – the 150 kDa dextran was given at 10 min and the 4 kDa dextran at 5 min before perfusion. The brain was separated into hemispheres, where one was sectioned and the other dissected, removing the cerebellum. The cerebrum was subsequently diluted 1:3 in PBS and homogenised. Dextran content in brain and terminal blood was measured with a spectrophotometer, and dextran extravasation was determined by calculating brain-to-blood ratio.

Brain tissue processing

Extracted mouse brains were either directly coronally cryosectioned or the cerebellum and brain hemispheres were separated, in which one hemisphere was cryosectioned and the other hemisphere was homogenised, and proteins were isolated with sequential sequences of extraction and centrifugation. Protein isolation was performed according to the following protocol: brain parts were homogenised in a PBS or TBS buffer and centrifuged at 16 000xg for 1 h. The supernatant was collected, and a portion of TBS supernatant was re-centrifuged at 100 000xg for 1 h and the supernatant was collected. Pellets from the first extraction were re-homogenised in TBST and centrifuged at 16 000xg for 1 h and the supernatant was collected. In the last step pellets were homogenised in formic acid and centrifuged at 16 000xg for 1 h with subsequent supernatant collection (Figure 8). In **paper I** and **IV**, A β species were sequentially isolated in PBS/TBS (soluble A β) fraction, TBST (membrane-associated A β) fraction, and formic acid (fibrillar A β).

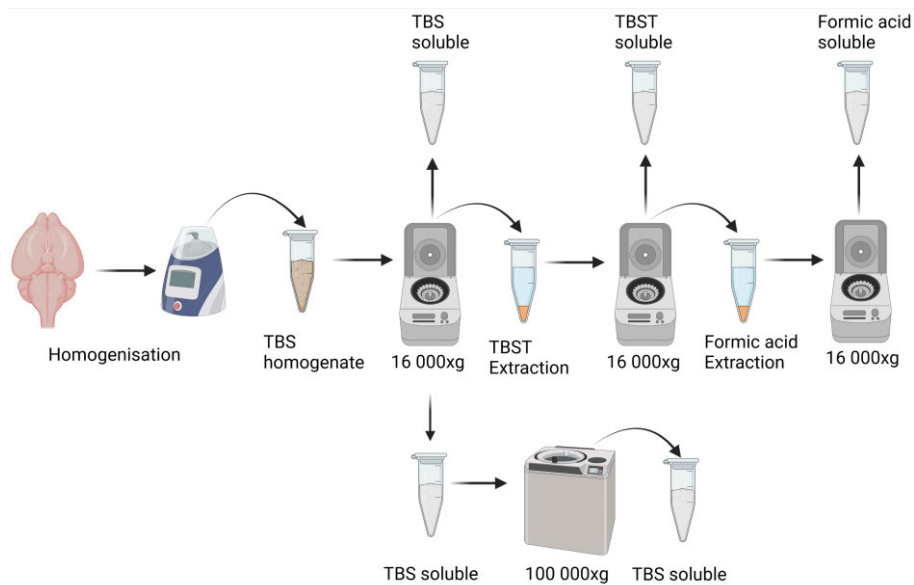


Figure 7. Schematic illustration of brain tissue processing and A β isolation. Brain was homogenised in TBS (PBS) buffer and centrifuged at 16 000xg. Supernatant containing soluble A β was split in two fractions, where one was further centrifuged at 100 000xg and the other was collected. Pellet from TBS fraction was TBST extracted and centrifuged at 16 000xg for 1h, and the supernatant containing membrane associate A β was collected. Lastly, TBST pellet was homogenised in formic acid, centrifuged at 16 000xg for 1h, and formic acid total A β was collected.

Autoradiography/emulsion autoradiography

Autoradiography is a method for detecting radioactive decay in a sample. Here, photostimulated luminescence was used to investigate *ex vivo* distribution in the brain of injected radiolabelled antibodies. To detect tissue radioactivity, incoming radioactivity is “stored” when Eu²⁺ is ionized and electrons are released, converting it to Eu³⁺. Electrons are “stored” in the atoms of the crystal lattice. Shining a laser releases the electron, which converts Eu³⁺ back to Eu²⁺, and in the process releases energy as light. The amount of emitted light is proportional to the amount of radioactivity and can be detected and produced as a digital image (autoradiogram). In **paper I-IV**, autoradiography was used to investigate the *ex vivo* spatial distribution in brain cryosections of injected radiolabeled antibodies.

In **emulsion radiography**, radioactivity is visualised in a liquid photographic film. The photographic film contains silver halide crystals, for example, silver bromide (AgBr), in a gelatin matrix. The emulsion is applied to the tissue section and the radioactivity ionises silver halide crystals, forming free electrons,

bromine ions, and clusters of silver atoms, also known as "latent image centres". Clustered silver atoms are selectively amplified during the development process, forming silver deposits seen as dark grains. Lastly, the amplified latent image centers are fixed. In **paper I**, emulsion autoradiography combined with Congo red staining was used to demonstrate the interaction of 3D6 with A β in CAA. In **paper II**, the degree of A β and vascular interactions of administered radioiodinated RmAb158-scFv8D3 and RmAb158 was quantified with emulsion autoradiography.

Tissue staining

Histological stainings are performed to visualise and examine the microscopic anatomical structure in a tissue section. Congo red is a member of the azo dye family that produces a red colour under alkaline conditions and can qualitatively be used to stain tissues and visualise amyloidosis by binding to its β -sheets.

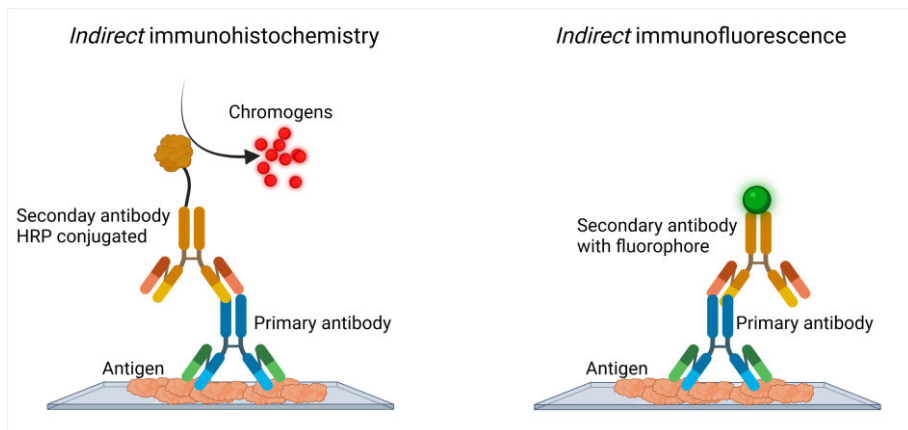


Figure 8. Depict *indirect* immunohistochemistry and *indirect* immunofluorescent staining of antigens in brain tissue.

In immunostaining, antibodies raised against specific antigens are used to detect tissue-residing molecules. In *direct* immunostaining, antibodies are conjugated with a detection molecule, usually a fluorophore or the enzyme horse radish peroxidase (HRP). *Indirect* staining is based on two sets of antibodies, a *primary* antibody binding to a tissue antigen and a *secondary* detection antibody recognising the primary antibody. In **paper II** and **III**, *indirect* immunohistochemistry and *indirect* immunofluorescence were used to detect brain tissue antigens (Figure 9). A β burden was investigated with Congo red stain (**paper I**), and polyclonal anti-A β 40 antibody (**paper II** and **III**). Vascular architecture was visualised with an anti-CD31 antibody (**paper II**).

Enzyme-linked immunosorbent assay (ELISA)

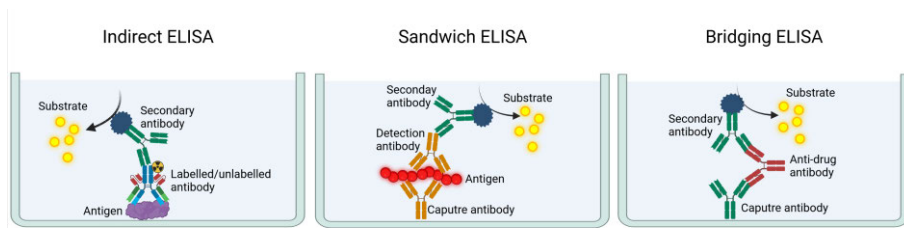


Figure 9. ELISA setup in described projects. The affinity of radiolabelled antibodies toward antigens was assessed with *indirect* ELISA. Protein concentration in brain homogenates was determined with *sandwich* ELISA. Presence of anti-drug antibodies in blood plasma was evaluated with *bridging* ELISA.

ELISA is an immunoassay in which antigens in solution from a complex biological sample can be detected and quantified using antibodies. Detection is based on a horseradish peroxidase (HRP) catalysed reaction of a chromogenic substance, which is detected with a spectrophotometer. The absorbance signal of antigen samples, correlated with absorbance of a serially diluted standard of known concentration, can determine antigen concentration in samples.

Depending on ELISA type, either a capture antibody or the antigen is immobilised in a 96-well plate. All ELISA experiments in described studies were performed with an *indirect*, *sandwich*, or *bridging* ELISA (Figure 10).

In **paper II** and **III** *indirect* ELISA was used as quality control of bispecific antibodies post-radiolabeling. A β and mTfR were immobilised and affinity was assessed with saturation assay comparing radiolabelled antibodies with unlabelled counterparts. In **paper I** and **IV**, brain A β load was quantified with different sandwich ELISAs. Soluble A β aggregates were quantified with a homogeneous ELISA using antibody 82E1 (**paper I**) or 3D6 (**paper IV**) (sharing the same N-terminal epitope), for both capture and detection. This setup ensures that only dimers or larger A β aggregates are detected due to self-epitope blocking. Total A β 40/42 was measured using polyclonal anti-A β 40/42 antibodies for capture and 82E1 or 3D6 for detection. In **paper IV**, the presence of ADA in plasma was detected with a bridging ELISA, in which capture and detection antibodies were the same as the treatment antibody. Since animals were immunised with the same antibody used for capture and detection, the resulting ADA in plasma will recognise the ELISA antibody pair and form a “bridge” (Figure 10).

Results and discussion

Paper I

Vascular A β deposition, or CAA, is a common histopathological finding among AD patients and is suggested to contribute to AD development, ultimately leading to neuronal loss. Evidence pinpoints vascular A β as an initiator of pro-inflammatory processes that ultimately increase BBB permeability, leading to dysregulated barrier transport and brain influx of blood residing molecules. From a neurotherapeutic perspective, the increased BBB permeability seen in AD could be beneficial for treatment delivery as it is permissive of a higher intra brain concentration of pharmacologically active substances. Moreover, the transient opening of the BBB has been explored as a possible way of increasing brain delivery of drugs.

In **paper I**, we examined whether the BBB of aged tg-ArcSwe mice is compromised due to abundant CAA. Furthermore, we assessed if a single dose of 3D6 (the murine version of Bapineuzimab) would increase the BBB permeability of dextrans. Early trials with the anti-A β antibody, Bapineuzimab, demonstrated that antibody treatment caused a dose-dependent increase in ARIA-E incidence in AD patients. Here, aged tg-ArcSwe mice were chosen due to advanced brain A β pathology with accompanying CAA in cortical and thalamic vessels. Tg-ArcSwe mice, 18 months old, and age-matched WT mice were administered a single dose of [125 I]3D6 or PBS as control. After three days, all animals received 4 kDa FITC-labelled dextrans and 150 kDa Antonia Red-labelled dextrans, and dextran extravasation was quantified as a dextran concentration brain-to-blood ratio, as measured by fluorescence. Brains were measured in a gamma counter to determine uptake of [125 I]3D6, and antibody distribution in brain tissue was investigated with autoradiography and emulsion autoradiography combined with Congo red staining to confirm the presence of A β pathology.

Generally, acute treatment with 3D6 did not increase extravasation of 4 kDa or 150 kDa dextrans, and brain-to-blood ratios were low in both tg-ArcSwe and WT mice. However, for the 150 kDa dextran, a minor correlation was observed between brain A β 40 and A β 42 concentration and dextran blood-to-brain ratio, where two mice with the highest brain A β concentration gave rise to the correlation, indicating increased BBB permeability. Brain uptake of

3D6 differed between transgenic and WT mice, such that transgenic mice had higher brain uptake ($P=0.015$) and an increased brain-to-blood ratio ($P=0.0072$). Autoradiography showed localised retention of [125 I]3D6 in cortex and thalamus of tg-ArcSwe mice, whereas WT mice were devoid of detectable antibody retention. Congo red staining and emulsion autoradiography confirmed accumulation of 3D6 in proximity of A β in CAA.

The BBB was relatively unaffected after a single dose of 3D6, although a slight correlation was seen between A β 40/42 and 150 kDa dextran, indicating the possibility of BBB perturbances in tg-ArcSwe mice. Though enticing, caution is warranted since only two tg-ArcSwe mice drove this correlation. It has been hypothesised that BBB breakdown, seen as ARIA, in AD immunotherapy is a prerequisite for delivering antibodies into the brain [176]. Although tg-ArcSwe mice had extensive CAA, the BBB was intact and 3D6 retention was higher than WT mice, indicating a certain degree of antibody brain entry and intra brain target engagement. Research has shown that perivascular transport pathways can transport antibodies in the brain [177]. Thus, the extensive CAA interaction of 3D6 could indicate that the antibody is transported via the perivascular space into the brain and that interactions with A β take place in certain vulnerable parts of brain vessels. In conclusion, we show that acute treatment with 3D6 does not negatively impact BBB permeability in tg-ArcSwe mice. Nevertheless, the pronounced 3D6 retention in CAA implies alternative intra brain transport pathways for antibodies.

Paper II

We have designed several bispecific antibody constructs that penetrate the BBB through RMT. The seminal construct was a chemically linked fusion protein of 8D3 and F(ab')₂ of mAb158 that could, when labelled with 124 I, be used as a PET ligand for imaging of soluble A β in the brain of A β mouse models [156]. The next iteration was a recombinantly produced version, RmAb158-scFv8D3, in which two scFv of 8D3 were fused to the light chain C-terminal of RmAb158. With this construct, brain uptake was improved, and in an acute immunotherapeutic study, RmAb158-scFv8D3 was ten times as efficient as RmAb158 in removing soluble A β . Since little is known about the long-term brain retention of antibodies, we expanded the time frame in **paper II** and explored RmAb158-scFv8D3's brain retention and distribution for a whole month in Tg-ArcSwe mice which have abundant A β pathology. We compared RmAb158-scFv8D3 against its parent construct, RmAb158, which is currently being evaluated in a clinical phase III trial for AD treatment. Furthermore, looking at high resolution how RmAb158-scFv8D3 and RmAb158 interact with intra-brain A β pathology would provide valuable information regarding treatment mechanisms and efficiency.

In **Paper II**, to enable investigation of brain distribution and blood pharmacokinetics over a month, RmAb158-scFv8D3 and RmAb158 were radiolabelled with the relatively long-lived radionuclide ^{125}I , (half-life 59.5 days). The study was conducted in aged tg-ArcSwe mice, which display abundant A β plaque pathology in the cortex, hippocampus and thalamus, and pronounced CAA, especially in the thalamus and cortex. Brain retention was addressed at multiple levels with different techniques. SPECT was used to explore brain uptake and antibody distribution at a gross level. Next, we utilised *ex vivo* autoradiography and emulsion autoradiography in combination with staining for A β and vascular marker (CD31) to pinpoint the exact location of injected radio-labelled antibodies.

Interestingly, there was a pronounced difference in brain uptake, distribution and blood pharmacokinetic profiles of RmAb158-scFv8D3 and RmAb158. Despite a 5.5 fold higher blood exposure of RmAb158, its bispecific variant displayed higher brain uptake and total brain exposure, highlighting RMT as a valuable tool for enhancing protein delivery into the brain. The rapid uptake and fast blood clearance of RmAb158-scFv8D3 translated into better SPECT imaging contrast with clear pathology interaction three days post-injection. Throughout the study, investigation with SPECT demonstrated that [^{125}I]RmAb158-scFv8D3 and [^{125}I]RmAb158 exhibited a profoundly different intra-brain distribution pattern, in which [^{125}I]RmAb158-scFv8D3 presented a uniform distribution pattern that was localised in areas known to harbour A β depositions, such as cortex, thalamus and hippocampus. On the other hand, at three days post-injection, brain uptake of [^{125}I]RmAb158 could not easily be visualised with SPECT. Most likely due to high blood background. Nevertheless, after six days, [^{125}I]RmAb158 SPECT scanning revealed a concentrated accumulation in what appeared to be the brain ventricles, which was more evident after two and four weeks. The spatial brain distribution of antibodies investigated with *ex vivo* autoradiography essentially confirmed SPECT findings. Tissue distribution of [^{125}I]RmAb158-scFv8D3 was uniform throughout the study and co-localised closely with A β 40 pathology. [^{125}I]RmAb158, on the other hand, displayed antibody retention as hot-spots throughout the study. Autoradiography of WT mice given [^{125}I]RmAb158-scFv8D3 or [^{125}I]RmAb158 did not show any retention after three days.

RmAb158 displayed a remarkably similar brain distribution pattern in tg-ArcSwe mice as observed with 3D6 in **paper I**, suggesting a shared uptake and distribution mechanism. Again, this was substantiated with emulsion autoradiography, which demonstrated high vascular retention [^{125}I]RmAb158 in CAA. A possible explanation for the observed vascular retention could be perivascular transport mechanisms where 3D6 and RmAb158 encounter and bind to perivascular A β . BBB breakage and leakage could also be a possible explanation for the hot spots, although this may be less likely since treatment

with 3D6 in tg-ArcSwe mice did not increase BBB permeability of large molecules. [^{125}I]RmAb158-scFv8D3, on the other hand, was substantially less associated with CAA and displayed a greater vascular escape, suggesting that RMT of anti-A β antibodies could reduce side effects like ARIA. Furthermore, high detailed assessment of parenchymal antibody distribution with emulsion autoradiography demonstrated a clear difference, where RmAb158-scFv8D3 exhibited a more pronounced cortical and hippocampal plaque interaction. Although RmAb158-scFv8D3 and RmAb158 displayed different brain distribution patterns, both had a similar half-time in the brain, underscoring a shared elimination mechanism. The similar brain half-life of RmAb158-scFv8D3 and RmAb158 could be attributed to a near-identical A β off-rate. Additional explanations could be phagocytosis by microglial cells or clearance via ISF flow.

In conclusion, in **paper II** we demonstrate and highlight the benefit of RMT for brain-directed immunotherapy. High-detail mapping of intra brain antibody distribution demonstrated that RMT resulted in lower CAA interaction and greater antibody interaction with parenchymal A β depositions, which would likely reduce ARIA and improve the effect of anti-A β treatment, respectively.

Paper III

In previous studies of A β imaging and antibody pharmacokinetics, we have successfully labelled BBB penetrating bispecific constructs with radioactive isotopes from the halogen group, including ^{124}I , ^{125}I , and ^{18}F . In **paper III** we expanded our radionuclide repertoire by labelling RmAb158-scFv8D3 with ^{111}In , a radiometal suitable for SPECT imaging. Our rationale was partly based on safety concerns with radioiodine, in which the thyroid readily takes up free radioiodine. Although iodine supplementation can block thyroidal uptake of radioiodine, this could be a concern in brain immunoimaging where a high dose is needed due to low BBB penetration (with RMT systems, approximately 1 % of the injected dose reaches the brain). Other interesting aspects of radiometals are prolonged cellular retention if the radiotracer is internalised. Another objective was to investigate potential alterations in brain retention and biodistribution of ^{111}In labelled RmAb158-scFv8D3.

The study design in **paper III** had a similar setup as in Hultqvist et al. [153], but here, we performed whole-body SPECT imaging to visualise antibody distribution to peripheral organs. To facilitate ^{111}In labelling, RmAb158-scFv8D3 was first conjugated with the chelators CHX-A"-DTPA, DOTA, or a DOTA-tetrazine variant. Brain uptake of ^{111}In labelled RmAb158-scFv8D3 was explored after 2 h in 4 months old WT mice, and after 72 h in 18 months old tg-ArcSwe mice and aged-match WT mice. Biodistribution was explored both with SPECT and *ex vivo* measurement of isolated organs. Blood samples

were collected to investigate blood pharmacokinetics of ^{111}In labelled RmAb158-scFv8D3, and brain distribution was investigated with *ex vivo* radiography.

Blood pharmacokinetic profiles and blood half-life were similar for all ^{111}In -labelled variants of RmAb158-scFv8D3 and corresponded with previously reported data from $^{124/125}\text{I}$ labelled RmAb158-scFv8D3 [153, 178] and 3D6-scFv8D3 [179]. At 2 h, brain uptake was similar for all variants ranging from 1-2% of injected dose, which resembles previously reported data on brain uptake of $^{124/125}\text{I}$ labelled RmAb158-scFv8D. Whole-body SPECT scanning indicated high liver, spleen, and bone accumulation of RmAb158-scFv8D3. Subsequent *ex vivo* measurement of organ retention confirmed SPECT data, with high retention in spleen, liver, and bone – with very high bone marrow retention. Interestingly, unlike what has been reported with radioiodinated RmAb158-scFv8D3, WT mice displayed unexpectedly high brain retention of ^{111}In labelled RmAb158-scFv8D3 after 72h. Nonetheless, tg-ArcSwe mice, compared with WT mice, had higher brain retention after 72h. *Ex vivo* brain autoradiography confirmed gamma measurement of the brain. In addition, autoradiography showed that distribution was uniform in both WT and tg-ArcSwe brains.

In **paper III** we demonstrate that a bispecific BBB penetrating antibody can successfully be ^{111}In labelled and retain its ability to be transported into the brain and bind its intra brain target. Although RmAb158-scFv8D3 successfully entered the brain, we demonstrated that ^{111}In labelling increased brain retention compared with its radioiodinated counterpart. In contrast to results in **paper II**, where the brains of WT mice administered radioiodinated RmAb158-scFv8D3 were completely devoid of activity after three days, the prolonged brain retention seen with ^{111}In label could be explained with several biological processes such as neuronal or microglial uptake of RmAb158-scFv8D3. Neurons have been reported to express the TfR [180, 181], and in our case, neuronal internalisation and subsequent degradation could explain the retention of ^{111}In . In **paper IV** we established that RmAb158-scFv8D3 is immunogenic due to its scFv8D3 moiety (rat-derived antibody fragment). Brain-residing activated microglia may recognize ^{111}In labelled RmAb158-scFv8D3 either in an A β immunocomplex or the scFv8D3 moiety as foreign, causing phagocytosis and intracellular degradation, ultimately resulting in microglia retention of ^{111}In . We also pinpointed bone marrow tissue as a place with high ^{111}In retention. Since the bone marrow's high iron demand is fulfilled by TfR mediated uptake, the observed ^{111}In retention is likely a result of normal TfR biology, where RmAb158-scFv8D3 is simply internalised and degraded. Hence, peripheral bone marrow uptake of bispecific constructs targeting TfR is unavoidable, although adjustment of binding valency and affinity toward TfR can alter peripheral uptake of the bispecific antibody. From the

perspective of radiopharmaceutical drugs, high bone marrow retention is a disadvantage due to the radiosensitivity of cells in the bone marrow.

Here, we expand and build on knowledge from **paper II**, further demonstrating a new intra brain retention pattern of RmAb158-scFv8D3. Furthermore, we highlight and underpin the need for careful investigations to understand the biology of the RMT systems currently being explored in brain-directed immunotherapy in AD and other CNS diseases.

Paper IV

Paper IV was based on knowledge gained from **paper II**, where we demonstrated that RmAb158-scFv8D3, compared with RmAb158, had a higher total brain exposure and greater interaction with parenchymal A β —highlighting that RMT could be utilised for improvement of brain-directed immunotherapy in AD. Furthermore, we have previously shown that a single injection of RmAb158-scFv8D3 is ten times as potent as RmAb158 in lowering soluble A β in tg-ArcSwe mice [182].

Combining insights from previous studies, we set out to evaluate if RmAb158-scFv8D3 is more efficient at removing A β than RmAb158. We explored this in three study regimes, targeting different pathological aspects of A β aggregation. All therapeutic studies were carried out in *App*^{NL-G-F} mice. The first study was similar to our previous acute therapy study in tg-ArcSwe mice [182], but conducted in 5 months old *App*^{NL-G-F} mice. Mice received a single dose of either RmAb158-scFv8D3, RmAb158 or PBS control, and the treatment period was three days. In the second treatment regimen, we attempted to target A β aggregates in 3 months old *App*^{NL-G-F} mice to inhibit seeding and further formation of A β plaque pathology. Animals received in total three injections (one every second day during one week) of RmAb158-scFv8D3, RmAb158, or PBS control followed by a period of 10 weeks without treatment. In the last treatment arm, the study was conducted in two phases. In phase 1, all mice were immunodepleted with an anti-CD4 antibody to enable repeated injection with RmAb158-scFv8D3 without eliciting an immune response directed to the antibody. In phase 2, mice were given weekly injections of RmAb158-scFv8D3, RmAb158, or PBS control for 8 weeks. A final diagnostic dose of [¹²⁵I]RmAb158-scFv8D3 was given to all treatment groups to correlate putative treatment effects with *ex vivo* brain uptake of [¹²⁵I]RmAb158-scFv8D3.

A second goal was to determine and potentially reduce the immunogenicity of RmAb158-scFv8D3 by repeatedly inoculating 4 months old WT mice with various antibody constructs. We assessed which factors or structural elements

of RmAb158-scFv8D3 would give rise to a humoral immune response resulting in anti-drug antibody (ADA) production. Since scFv8D3 is a rat-derived antibody fragment, we first attempted to reduce the immunogenicity by changing amino acids at positions predicted to lower MCHII binding affinity, thus lowering CD4 T-cell mediated immune response. Subsequently, we addressed whether a mouse chimeric 8D3 would escape detection of the immune system as it lacks the peptide linkers used between antibody domains of RmAb158-scFv8D3. We also assessed the influence of protein aggregation by testing an aggregation free preparation of RmAb158-scFv8D3. Lastly, the antibody's Fc region's influence and valancy of mTfR binding was assessed with a di-scFv fragment, lacking an Fc domain and having monovalent binding to mTfR.

Although we have shown that RmAb158-scFv8D3 successfully enters the brain and can be used as a PET ligand, not much is known about its immunogenic potential. Repeated injections lowered blood exposure which decreased the brain uptake of RmAb158-scFv8D3. We subsequently confirmed the presence of ADA, thus demonstrating a host reaction toward RmAb158-scFv8D3. Furthermore, creating a mutant version with predicted lower MCHII binding affinity did not lower the ADA response. In addition, chimeric 8D3, aggregation free RmAb158-scFv8D3 did not lower ADA response. Interestingly, treatment with di-scFv3D6-8D3 resulted in a less severe ADA response. Immunised and naïve mice had similar blood retention and spleen uptake. Further, brain uptake of di-scFv3D6-8D3 in immunised mice were higher compared with mice immunised with mutated or aggregation free RmAb158-scFv8D3. In conclusion, RmAb158-scFv8D3 elicited a humoral immune response and attempts to lower its immunogenicity were unsuccessful. Still, the di-scFv constructed had an attenuated ADA response indicating that the Fc region or mTfR binding valancy partly explains the immunogenicity of RmAb158-scFv8D3. We circumvented ADA formation by depleting CD4⁺ T-cells in mice and thus allowing repeated injection of RmAb158-scFv8D3.

Comparing RmAb158-scFv8D3's treatment efficacy against RmAb158 in multiple treatment regimes. We have previously shown that a single dose of RmAb158-scFv8D3 is ten times more potent than RmAb158 in removing soluble A β [182]. Here, single-dose treatment did not lower soluble A β in *App*^{NL-G-F} mice in either of the treatment groups compared with PBS control. The exact mechanism why single dose treatment failed is unknown. A possible explanation could be the Iberian mutation, which increases A β 42, shifting the aggregation pathway towards insoluble A β , thus lowering soluble A β concentration. Indeed, a comparison showed that *App*^{NL-G-F} had substantially lower levels of soluble A β aggregates compared to tg-ArcSwe mice. Next, we attempted to prolong time to A β deposition by removing A β seeds at a young age. Significant treatment effects was seen in A β 42 (main A β pool for *App*^{NL-G-F}) in hippocampus for RmAb158 (p<0.05) and a trend was seen for

RmAb158-scFv8D3 ($p=0.066$) . In cortex a trend was seen for RmAb158 in lowering A β 42.

In the last treatment regimen, initial CD4 cell depletion successfully lowered ADA response towards RmAb158-scFv8D3. Interestingly, repeated treatment with RmAb158-scFv8D3 resulted in a dose-dependent shift in blood and plasma kinetics of the final diagnostic dose of [125 I]RmAb158-scFv8D3, where high dose treatment had lowest concentration in plasma but highest concentration in whole blood. Repeated RmAb158 treatment did not alter blood or plasma kinetics. Observed alterations in blood and plasma kinetics correlated with brain uptake of [125 I]RmAb158-scFv8D3, where the high dose group had the lowest brain uptake. The expected result was that low brain uptake of [125 I]RmAb158-scFv8D3 would indicate a reduced brain A β burden as a result of successful treatment. Indeed, RmAb158-scFv8D3 and RmAb158 displayed a statistical significant reduction in total A β 1-42, the most abundant A β species in the brain, but the difference in brain concentration of the diagnostic [125 I]RmAb158-scFv8D3 rather reflected a treatment induced difference in tracer pharmacokinetics. In line with the two first studies, neither of the long-term treatment groups displayed reduction of soluble A β .

Although we have shown in **paper II** that RMT increases antibody interaction with parenchymal A β , long-term treatment with RmAb158-scFv8D3 did not demonstrate any added benefits in lowering of A β despite successful mitigation of ADA response. There are several potential explanations for the observed lack of treatment effects with repeated RmAb158-scFv8D3 administration. One possibility could be ascribed to lowering of bioavailability due to increased blood cell expression of TfR that sequesters RmAb158-scFv8D3 in the peripheral circulation. The observed increase in blood retention in the high dose treatment group supports this. Another mechanism leading to a reduced brain uptake of RmAb158-scFv8D3 could be a higher concentration of soluble truncated TfR in plasma, which binds to the 8D3 fragment, blocking TfR mediated BBB transport. It is also possible that repeated RmAb158-scFv8D3 administration resulted in reduced TfR expression on the BBB, and thus lowered brain delivery, resulting in loss of treatment effects. Further, it has been suggested that microglial phagocytosis of A β -antibody complexes is the main mechanisms to mediate A β clearance in AD immunotherapy [136]. Here, it is possible that the scFv moiety lowers binding of the RmAb158-scFv8D3-A β complex to Fc gamma receptors on microglia, leading to blunted activation of phagocytosis.

Knowledge gained in **paper I, II** and **III** led to the project in **paper IV**. One of the main findings in **paper II** was that BBB RMT increased brain uptake of bispecific antibodies, leading to a greater parenchymal A β interaction, likely translating into better therapeutic effects. We further explored intra

brain distribution of RmAb158-scFv8D3 by labelling the antibody with an intracellular residualizing tag (^{111}In) (**paper III**). Results showed increased cellular retention in the brain, which could be interpreted as a possible treatment mechanism where $\text{A}\beta$ -RmAb158-scFv8D3 complex is phagocytosed by, for example, microglia. However, it could also reflect a previously undetected interaction with neuronal TfR that could in fact reduce interactions with $\text{A}\beta$ and thereby therapeutic effects of the bispecific antibody.

Synthesis of the above-described projects warranted a comprehensive investigation addressing if a long-term treatment study with repeated injection of the bispecific antibody, RmAb158-scFv8D3, would result in additional improvement in lowering $\text{A}\beta$ of the brain. We found out that RmAb158-scFv8D3 was immunogenic, resulting in a humoral immune response leading to ADA production. CD4^+ T-cell immunodepleting mitigated the ADA response, enabling repeated injection RmAb158-scFv8D3, and thus an immunotherapy study was initiated. Although we managed to control the ADA response, long-term treatment with RmAb158-scFv8D3 did not out-perform RmAb158.

Conclusion and future perspectives

A considerable amount of resources have been invested in the development of A β targeting antibodies, and until recently, with limited success. The lack of success of the many tested antibodies could partially be explained by a failure to target the most pathologically relevant aggregation state of A β . Furthermore, several clinical trials with anti-A β antibodies have highlighted safety concerns such as vascular disturbances seen as ARIA, which are believed to result from antibody interaction of vascular A β deposits. A problem in brain directed immunotherapy is that the BBB reduces brain uptake of antibodies. Although problematic, the identification of several transcellular transport systems at the BBB has prompted the development of engineered bispecific antibodies that utilize these systems for increased brain uptake.

In this thesis, we assessed the BBB integrity in an A β mouse model with and without immunotherapy. Furthermore, we explored the intra brain distribution and peripheral biodistribution of a bispecific BBB penetrating anti-A β antibody and assessed whether transport over the BBB translated into a more significant reduction of brain A β in a transgene A β mouse model. Clinical studies with *Bapineuzumab* have demonstrated that AD patients develop ARIA [183]. Here, a single dose of 3D6 (murine *Bapineuzumab*) did not increase BBB permeability. However, 3D6 was highly retained in vascular A β deposits, suggesting BBB breakdown is not a prerequisite for intra brain targeting of antibodies (**paper I**). Next, radiolabeling a bispecific antibody with ^{125}I (**paper II**) or ^{111}In (**paper III**) made it possible to investigate its distribution in brain and peripheral organs with SPECT. Bispecific antibodies labelled with ^{125}I and ^{111}In entered the brain and had a uniform intra brain distribution pattern. Interestingly, ^{111}In labelled bispecific antibody given to WT mice had unexpectedly prolonged brain retention. Furthermore, ^{111}In labelled antibodies had a high uptake in the bone marrow (**paper III**). ^{125}I labelling enabled prolonged *in vivo* investigation with SPECT which showed retention of the bispecific antibody coincided with areas harbouring A β pathology. Detailed *ex vivo* examination showed that the bispecific antibody displays greater vascular escape and more avid A β plaque binding, lowering the risk of vascular disturbances and perhaps improving brain-directed immunotherapy (**paper II**). The difference in biodistribution of RmAb158-scFv8D3 labelled with ^{125}I and ^{111}In is

probably due to different intracellular retention properties of iodine and metals, in combination with the biology of the TfR receptor. Careful consideration is warranted when choosing the RMT system to transport radiometal labelled bispecific antibodies. In the final project (**paper IV**) we set out to evaluate the bispecific antibody in comparison to its unmodified parental counterpart in a long-term immunotherapy study in an A β mouse model. We found that RMT delivery of an antibody did not improve treatment efficacy, and brain A β levels were comparable with that of mice receiving regular antibody treatment. We hypothesised that the lack of improved treatment effect with the bispecific antibody could be due to alteration in its blood pharmacokinetics or in its design, where structural properties reduce phagocytosis of antibody-antigen complexes. Additional structural problems with the bispecific antibody, possibly explaining the prolonged brain retention (**paper III**) and altered pharmacokinetics after repeated injections (**paper IV**), could be attributed to the administered high dose. It is possible that both scFv8D3 fragments attached to the antibody engage with and cluster mTfR in a dose dependent manner.

The recent FDA conditional approval of *aducanumab* (Aduhelm) has invigorated and renewed interest in brain directed immunotherapy for treatment of AD. Although successful, AD immunotherapy faces challenges such as low brain uptake that requires a high dose to achieve the desired treatment effect. Another dose-related challenge is vascular disturbances. Here we demonstrate that RMT of anti-A β antibodies seems to reduce vascular A β binding and with increased parenchymal A β , likely providing benefits in immunotherapy. And indeed, Roche is now evaluating a bispecific version of Gantenerumab, targeting human TfR, for treatment of early AD [184].

However, bispecific antibodies present a host of new challenges that need to be addressed. Careful consideration regarding the structure of the bispecific antibody is of importance. For example, the structural placement of RMT targeting moiety could reduce potential treatment effect by reducing Fc γ mediated phagocytosis. Another important structural factor is valancy of mTfR interaction. As such it would be interesting to assess treatment efficacy of and biodistribution of a bispecific antibody with a “true” monovalant mTfR interaction. To date there is no clear *in vivo* evidence of how anti-A β antibodies lower brain A β , which needs to be extensively investigated to design strategies to achieve optimal treatment efficacy. Furthermore, the biology of the targeted RMT system needs to be carefully investigated. This is of particular importance when using radiolabelled bispecific antibodies targeting the TfR. Bone marrow tissue is highly radiosensitive due to rapidly dividing hematopoietic cells. These cells have a high iron need and thus express high levels of TfR, and utilisation of TfR targeting radiolabelled antibodies would greatly increase the radioactive dose, which is even more problematic with residulising radiometals.

Populärvetenskaplig sammanfattning

Globalt lever ungefär 50 miljoner människor med demens vilket är en siffra som förväntas stiga till 150 miljoner till år 2050. Alzheimers sjukdom är den vanligaste formen av demens och står för 70% av alla fall. Sjukdomsmekanismerna som ger upphov till Alzheimers sjukdom beror på aggregering av proteiner i hjärnan. Framförallt är det proteinet amyloid-beta ($A\beta$) som bildar ”plack” utanför hjärncellerna eller Tau-proteinet som bildar ”proteinnystan” inuti nervceller. Tillväxten av proteinaggregaten startar ogynnsamma processer i hjärnan så som inflammation, synapsstörningar och slutligen nervcells-död. Oroväckande är att dessa processer startar decennier innan symptomdebut och fram tills nyligen fanns det endast symptomlindrande behandling.

Blod-hjärnbarriären är en speciell vaskulär struktur i hjärnan som begränsar inflödet av potentiellt farliga molekyler till hjärnan. Från ett läkemedelsperspektiv är blod-hjärnbarriären ett hinder då den blockerar passage av läkemedel in i hjärnan. Då blod-hjärnbarriären även förhindrar upptag av livsnödvändiga näringsämnen finns det ett flertal transportproteiner som faciliterar transport av näringsämnen in i hjärnan. Forskare har upptäckt att genom att låta läkemedelsmolekyler åka snålskjuts med dessa transportproteiner kan man kraftigt öka införseln av läkemedel i hjärnan. Ett av dessa transportsystem är transferrinreceptorn som bland annat transporterar järn in till hjärnan, och läkemedelsbolag och forskargrupper världen över har använt detta för transport av proteinbaserade läkemedel in i hjärnan.

I denna avhandling har jag utvärderat antikroppsläkemedel mot $A\beta$. För att kunna fastställa behandlingseffekt och eventuella biverkningar så använder vi oss av genetiskt modifierade möss som producerar mänskligt $A\beta$ i hjärnan. Mer specifikt så har jag jämfört en bispecifik antikropp (som binder till både transferrinreceptorn och $A\beta$) med en omodifierad variant (som enbart binder till $A\beta$). Antikropparna märktes med radioaktiva spårämnen för att kunna mäta hjärnupptag och se distributionen i mössen.

I delarbete I utvärderade vi om blod-hjärnbarriären är påverkad och läcker i en $A\beta$ -musmodell, antagligen till följd av patologin eller p.g.a antikroppsbehandling mot $A\beta$. För att kunna fastställa att närvaron $A\beta$ -patologi orsakar skada på blod-hjärnbarriären så inkluderade vi ockspö möss utan $A\beta$ som kontroll. Generellt var blod-hjärnbarriären opåverkad och ingen skillnad kunde

ses mellan A β -möss och kontrollmöss. Dock observerades en trend där antikroppstillförsel orsakade ett litet läckage hos möss med högst koncentration av A β i hjärnan. När vi analyserade antikroppsdistributionen i detalj så påträffades en stor del av antikropparna i blodkärl som innehöll A β .

I delarbete **II** och **III** utvärderade vi hjärnupptag och kroppsdistribution av en bispecifik antikropp. I delarbete **II** märktes den bispecifika antikroppen och en motsvarande omodifierad antikropp med radioaktivt jod och hjärnupptag och vävnadsdistribution jämfördes i A β -möss. Den omodifierade antikroppens distribution liknade den i delarbete **I** och påträffades i blodkärl med A β , men även i viss mång kring A β -plack inne i hjärnan. Hjärndistributionen för den bispecifika antikroppen, som aktivt transporteras in i hjärnan, var bättre och påträffades till mindre del i blodkärl. Intressant, och även gynnsamt ur ett behandlingsperspektiv, så påträffades den bispecifika antikroppen till större del kring A β plack i hjärnan. I den efterföljande studien kopplades radioaktivt indium till den bispecifika antikroppen. Om indium, till skillnad från jod, tas upp av en cell så stannar det kvar längre och därmed kan vi undersöka huruvida den bispecifika antikroppen tas upp av celler i hjärnan. Den bispecifika antikroppen utvärderades i A β -möss och kontrollmöss utan A β . Vi fann att antikroppen som var märkt med indium kom in i hjärnan precis som vi observerat för de tidigare jod-märkta antikroppen. Dock hade möss utan A β en oväntat hög antikroppsretention vilket tyder på cellupptag.

I delarbete **IV** utvärderade vi den bispecifika och den omodifierade antikroppen i ett fleral olika behandlingstrategier med målet att reducera A β i hjärnan. En singeldos med båda antikropparna påvisade inga förändringar i det mest lösliga A β . I nästa behandling administrerades totalt 3 doser med 2 dagars mellanrum mellan varje dos. Vi fann en trend där möss som behandlades med den bispecifika antikroppen hade mindre A β tio veckor efter avslutad behandling. I den sista studien dämpades immunförsvaret för att kunna göra upprepade injektioner med den bispecifika antikroppen under en längre tid. Trots ökat hjärnupptag, var den bispecifika antikroppen inte bättre än den omodifierade versionen. Möjliga orsaker kan vara strukturella skillnader mellan antikropparna där den bispecifika antikroppen, trots ökat upptag, inte förmår avlägsna A β . En annan orsak kan vara den förändrade bloddistribution där den bispecifika antikroppen binder till och fångas upp av blodceller.

Utvecklingen av bispecifika antikroppar som penetrerar blod-hjärnbarriären har stor potential för behandling av olika sjukdomar i hjärnan. I denna avhandling visar jag att en bispecifik antikropp som aktivt transporteras in i hjärnan hittar och binder till sitt mål, A β , och skulle kunna användas som behandling i Alzheimers sjukdom. Dock, trots ökat hjärnupptag, så var den bispecifika antikroppen marginellt bättre än sin omodifierade variant i en långtidsbehandlingsstudie. För att optimera och förbättra behandling bör framtida studier undersöka hur bispecifika antikroppsstruktur påverkar behandlingseffekter.

Acknowledgement

This thesis was performed at the Department of Public Health and Caring Sciences, Molecular Geriatrics group, Rudbeck Laboratory, Uppsala University, Sweden. I would like to thank for the financial support from the Swedish Research Council, Alzheimersfonden, Hjärnfonden, Torsten Söderbergs stiftelse, Åke Wibergs stiftelse, Åhlénstiftelsen, Magnus Bergwalls stiftelse, Stiftelsen för gamla tjänarinnor, Stohnes stiftelse, Hedlunds stiftelse, Goljes stiftelse, Konung Gustaf V:s och Drottning Victorias frimurarestiftelse and VINNOVA.

To my supervisors, **Dag**, **Stina**, and **Paul**. Without support from you guys, this would not have been possible. I would like to thank my main supervisor **Dag** (who started as my co-supervisor) for accepting me as his first PhD student. I appreciate your support during my PhD and that you always were available (even 23:30 on WhatsApp for a scientific discussion). Your knowledge of the dementia field is awe-inspiring and your skill with the multipipette is legendary. Not only are you a skilful researcher, but you are also a good musician. But most importantly, you are a good-hearted and decent person that is pleasant to work with. One could not have wished for a better “boss”, and I have learned a lot from you. My co-supervisor **Stina** (who started as my main supervisor) I contacted you at the end of my master's program, looking for a place to do my master's project. I was thrilled that you accepted me and that is how I started my journey towards becoming a researcher. Much of what was said about Dag is true for you too, Stina. What I admire about you is your organisational skills and effectiveness. I think I picked it up a bit, but there is still room for improvement. **Paul**, you have been a bedrock and provided excellent language support. Your knowledge is vast in microscopy and image analysis and in science overall.

Anish, aka the sausage man, it has been a pleasure having you as an office neighbour. Humor-wise we are similar and we shared many good laughs. Just a few more months and you will also enjoy freedom! **Silvio**, aka the mountain boy, I never met such an unlucky person, with conditions ranging from traumatic foot injuries to strange viral infections. It was a blast having you in the lab and I enjoyed all the GTs we had. **Rebecca**, you will now become the PET group's senior PhD student. It is a big responsibility, but I am sure you will

manage it perfectly. Furthermore, I still have not tried Norwegian pancakes and thanks for all brain homogenisation. To the Marie Curie students. **Gillian**, friendly and sweet as maple syrup, I hope your projects will bear fruit =). **Mengfei**, you have the most friendly morning waving. As you are the most hardworking person in the lab, please remember to take a break! And **Eva**, now you need to care for Dag when I am gone. Also, I will miss your friendly smile and unique laugh. **Lill-Tobbe**, you are now the man of the microscope room. Take good care of the microscope. Furthermore, I will miss your homebrew beer. **Jinar**, or queen of inflammation, you are like a walking Wikipedia page of neuroinflammation. I really enjoyed warming lunchroom seats for you and all our conversations. **Sahar**, probably the most thoughtful person in the lab. I appreciated your support during my final weeks of thesis writing. To the Finns. **Ulrika**, I could not have asked for a better neighbour. You always made sure I remembered to take a fika. **Johanna**, thanks for sharing your vast chromatography knowledge and for letting me use your hairdryer. **Emma**, vi medicinare håller ihop. It is great to hear that you will come back to the lab. I wish you all the best for the rest of your PhD. Central and southern Europeans, it is such a shame that I moved to the other side of the lab. **Agnieszka**, thanks for all the delicious meat you brought for our kick-offs. **Evangelos**, I think you are next in line, and like Anish, soon you can enjoy your freedom. **Chiara**, it was great having you as company in the cell lab. I attribute the lack of infections in my cell cultures to your presence.

Ximena, without you in the lab no research would be possible. Also, your tiramisu is amazing. **Joakim**, not only are you a great researcher, you are also funny. And a good attire. When it comes to protein aggregation and shoes you are my inspiration. **Anna**, you are the queen of astrocytes. I liked the Gotland stories you told during lunch and coffee breaks. **Vilmantas**, without you nothing IT-related would work. I appreciate all help you gave me.

Thanks to my students, **Viktorija** and **Isaline**, for your enthusiasm and contribution to my projects. I know it was not easy handling so much ADA (I feel the same!).

To the ProDDe gang. **Greta**, thanks for teaching me the nuts and bolts on reducing the MCHII affinity of peptide fragments. Also, it is great to have person from northern Uppland close by. And a big thank you to **Nicole**, **Jamie**, **Canan** and the rest of the group. **Fadi**, I see a bright future for you and many thanks for all the romantic troubleshooting you provided.

Serhii, your patience, guidance and hospitality was greatly appreciated. You are truly a great teacher and researcher. I hope to soon see you again. Many thanks prof. **Thomas Lars Andersen** and **Kasper Bendix Johnsen** for hosting me at DTU.

Last but not least, thanks to all former colleagues I worked with: **Tsong, Leire, Elisabeth, Linn, Agata, Sara, Maria, Martin, and Gabriel.**

References

1. Organization GWH: Risk reduction of cognitive decline and dementia: WHO guidelines. 2019.
2. Cipriani G, Dolciotti C, Picchi L, Bonuccelli U: Alzheimer and his disease: a brief history. *Neurol Sci* 2011, 32(2):275-279.
3. Selkoe DJ: Alzheimer's disease is a synaptic failure. *Science* 2002, 298(5594):789-791.
4. Serrano-Pozo A, Frosch MP, Masliah E, Hyman BT: Neuropathological alterations in Alzheimer disease. *Cold Spring Harb Perspect Med* 2011, 1(1):a006189.
5. Pawlowski M, Meuth SG, Duning T: Cerebrospinal Fluid Biomarkers in Alzheimer's Disease-From Brain Starch to Bench and Bedside. *Diagnostics (Basel)* 2017, 7(3).
6. Takahashi RH, Nagao T, Gouras GK: Plaque formation and the intraneuronal accumulation of beta-amyloid in Alzheimer's disease. *Pathol Int* 2017, 67(4):185-193.
7. Walsh DM, Teplow DB: Alzheimer's disease and the amyloid beta-protein. *Prog Mol Biol Transl Sci* 2012, 107:101-124.
8. Crews L, Masliah E: Molecular mechanisms of neurodegeneration in Alzheimer's disease. *Hum Mol Genet* 2010, 19(R1):R12-20.
9. Chow VW, Mattson MP, Wong PC, Gleichmann M: An overview of APP processing enzymes and products. *Neuromolecular Med* 2010, 12(1):1-12.
10. Finder VH, Glockshuber R: Amyloid-beta aggregation. *Neurodegener Dis* 2007, 4(1):13-27.
11. Dickson TC, Vickers JC: The morphological phenotype of beta-amyloid plaques and associated neuritic changes in Alzheimer's disease. *Neuroscience* 2001, 105(1):99-107.
12. Querol-Vilaseca M, Colom-Cadena M, Pegueroles J, Nunez-Llaves R, Luque-Cabecerans J, Munoz-Llahuna L, Andilla J, Belbin O, Spires-Jones TL, Gelpi E *et al*: Nanoscale structure of amyloid-beta plaques in Alzheimer's disease. *Sci Rep* 2019, 9(1):5181.
13. Thal DR, Rub U, Schultz C, Sassin I, Ghebremedhin E, Del Tredici K, Braak E, Braak H: Sequence of A β -protein deposition in the human medial temporal lobe. *J Neuropathol Exp Neurol* 2000, 59(8):733-748.
14. Thomsen MS, Routh LJ, Moos T: The vascular basement membrane in the healthy and pathological brain. *J Cereb Blood Flow Metab* 2017, 37(10):3300-3317.
15. Arvanitakis Z, Capuano AW, Leurgans SE, Buchman AS, Bennett DA, Schneider JA: The Relationship of Cerebral Vessel Pathology to Brain Microinfarcts. *Brain Pathol* 2017, 27(1):77-85.

16. Carrano A, Hoozemans JJ, van der Vies SM, van Horssen J, de Vries HE, Rozemuller AJ: Neuroinflammation and blood-brain barrier changes in capillary amyloid angiopathy. *Neurodegener Dis* 2012, 10(1-4):329-331.
17. Prelli F, Castano E, Glenner GG, Frangione B: Differences between vascular and plaque core amyloid in Alzheimer's disease. *J Neurochem* 1988, 51(2):648-651.
18. Suzuki N, Iwatsubo T, Odaka A, Ishibashi Y, Kitada C, Ihara Y: High tissue content of soluble beta 1-40 is linked to cerebral amyloid angiopathy. *Am J Pathol* 1994, 145(2):452-460.
19. Erickson MA, Banks WA: Blood-brain barrier dysfunction as a cause and consequence of Alzheimer's disease. *J Cereb Blood Flow Metab* 2013, 33(10):1500-1513.
20. Palmeri A, Ricciarelli R, Gulisano W, Rivera D, Rebosio C, Calcagno E, Tropea MR, Conti S, Das U, Roy S *et al*: Amyloid-beta Peptide Is Needed for cGMP-Induced Long-Term Potentiation and Memory. *J Neurosci* 2017, 37(29):6926-6937.
21. Cairns NJ, Farr SA: The role of amyloid-beta in the regulation of memory. *Biochem Pharmacol* 2014, 88(4):479-485.
22. Kagan BL, Jang H, Capone R, Teran Arce F, Ramachandran S, Lal R, Nussinov R: Antimicrobial properties of amyloid peptides. *Mol Pharm* 2012, 9(4):708-717.
23. Hardy JA, Higgins GA: Alzheimer's disease: the amyloid cascade hypothesis. *Science* 1992, 256(5054):184-185.
24. McLean CA, Cherny RA, Fraser FW, Fuller SJ, Smith MJ, Beyreuther K, Bush AI, Masters CL: Soluble pool of Abeta amyloid as a determinant of severity of neurodegeneration in Alzheimer's disease. *Ann Neurol* 1999, 46(6):860-866.
25. Aizenstein HJ, Nebes RD, Saxton JA, Price JC, Mathis CA, Tsopelas ND, Ziolkowski SK, James JA, Snitz BE, Houck PR *et al*: Frequent amyloid deposition without significant cognitive impairment among the elderly. *Arch Neurol* 2008, 65(11):1509-1517.
26. Shankar GM, Li S, Mehta TH, Garcia-Munoz A, Shepardson NE, Smith I, Brett FM, Farrell MA, Rowan MJ, Lemere CA *et al*: Amyloid-beta protein dimers isolated directly from Alzheimer's brains impair synaptic plasticity and memory. *Nat Med* 2008, 14(8):837-842.
27. Lesne S, Koh MT, Kotilinek L, Kaye R, Glabe CG, Yang A, Gallagher M, Ashe KH: A specific amyloid-beta protein assembly in the brain impairs memory. *Nature* 2006, 440(7082):352-357.
28. Hartley DM, Walsh DM, Ye CP, Diehl T, Vasquez S, Vassilev PM, Teplow DB, Selkoe DJ: Protofibrillar intermediates of amyloid beta-protein induce acute electrophysiological changes and progressive neurotoxicity in cortical neurons. *J Neurosci* 1999, 19(20):8876-8884.
29. Saido T, Leissring MA: Proteolytic degradation of amyloid beta-protein. *Cold Spring Harb Perspect Med* 2012, 2(6):a006379.
30. Huang SM, Mouri A, Kokubo H, Nakajima R, Suemoto T, Higuchi M, Staufenbiel M, Noda Y, Yamaguchi H, Nabeshima T *et al*: Neprilysin-sensitive synapse-associated amyloid-beta peptide oligomers impair neuronal plasticity and cognitive function. *J Biol Chem* 2006, 281(26):17941-17951.

31. Carpentier M, Robitaille Y, DesGroseillers L, Boileau G, Marcinkiewicz M: Declining expression of neprilysin in Alzheimer disease vasculature: possible involvement in cerebral amyloid angiopathy. *J Neuropathol Exp Neurol* 2002, 61(10):849-856.
32. Lee CY, Landreth GE: The role of microglia in amyloid clearance from the AD brain. *J Neural Transm (Vienna)* 2010, 117(8):949-960.
33. Sollvander S, Nikitidou E, Brolin R, Soderberg L, Sehlin D, Lannfelt L, Erlandsson A: Accumulation of amyloid-beta by astrocytes result in enlarged endosomes and microvesicle-induced apoptosis of neurons. *Mol Neurodegener* 2016, 11(1):38.
34. Tarasoff-Conway JM, Carare RO, Osorio RS, Glodzik L, Butler T, Fieremans E, Axel L, Rusinek H, Nicholson C, Zlokovic BV *et al*: Clearance systems in the brain-implications for Alzheimer disease. *Nat Rev Neurol* 2015, 11(8):457-470.
35. Van Cauwenbergh C, Van Broeckhoven C, Sleegers K: The genetic landscape of Alzheimer disease: clinical implications and perspectives. *Genet Med* 2016, 18(5):421-430.
36. Mullan M, Crawford F, Axelman K, Houlden H, Lilius L, Winblad B, Lannfelt L: A pathogenic mutation for probable Alzheimer's disease in the APP gene at the N-terminus of beta-amyloid. *Nat Genet* 1992, 1(5):345-347.
37. Scheuner D, Eckman C, Jensen M, Song X, Citron M, Suzuki N, Bird TD, Hardy J, Hutton M, Kukull W *et al*: Secreted amyloid beta-protein similar to that in the senile plaques of Alzheimer's disease is increased in vivo by the presenilin 1 and 2 and APP mutations linked to familial Alzheimer's disease. *Nat Med* 1996, 2(8):864-870.
38. Nilsberth C, Westlind-Danielsson A, Eckman CB, Condron MM, Axelman K, Forsell C, Stenh C, Luthman J, Teplow DB, Younkin SG *et al*: The 'Arctic' APP mutation (E693G) causes Alzheimer's disease by enhanced A β protofibril formation. *Nat Neurosci* 2001, 4(9):887-893.
39. Saito T, Matsuba Y, Mihira N, Takano J, Nilsson P, Itohara S, Iwata N, Saido TC: Single App knock-in mouse models of Alzheimer's disease. *Nat Neurosci* 2014, 17(5):661-663.
40. Aamodt EJ, Williams RC, Jr.: Microtubule-associated proteins connect microtubules and neurofilaments in vitro. *Biochemistry* 1984, 23(25):6023-6031.
41. Goedert M, Spillantini MG, Jakes R, Rutherford D, Crowther RA: Multiple isoforms of human microtubule-associated protein tau: sequences and localization in neurofibrillary tangles of Alzheimer's disease. *Neuron* 1989, 3(4):519-526.
42. Brunello CA, Merezko M, Uronen RL, Huttunen HJ: Mechanisms of secretion and spreading of pathological tau protein. *Cell Mol Life Sci* 2019.
43. Gao YL, Wang N, Sun FR, Cao XP, Zhang W, Yu JT: Tau in neurodegenerative disease. *Ann Transl Med* 2018, 6(10):175.
44. Scholl M, Lockhart SN, Schonhaut DR, O'Neil JP, Janabi M, Ossenkoppele R, Baker SL, Vogel JW, Faria J, Schwimmer HD *et al*: PET Imaging of Tau Deposition in the Aging Human Brain. *Neuron* 2016, 89(5):971-982.

45. Ossenkoppele R, Schonhaut DR, Scholl M, Lockhart SN, Ayakta N, Baker SL, O'Neil JP, Janabi M, Lazaris A, Cantwell A *et al*: Tau PET patterns mirror clinical and neuroanatomical variability in Alzheimer's disease. *Brain* 2016, 139(Pt 5):1551-1567.
46. Mattsson-Carlgren N, Andersson E, Janelidze S, Ossenkoppele R, Insel P, Strandberg O, Zetterberg H, Rosen HJ, Rabinovici G, Chai X *et al*: Abeta deposition is associated with increases in soluble and phosphorylated tau that precede a positive Tau PET in Alzheimer's disease. *Sci Adv* 2020, 6(16):eaa2387.
47. Shin WS, Di J, Cao Q, Li B, Seidler PM, Murray KA, Bitan G, Jiang L: Amyloid beta-protein oligomers promote the uptake of tau fibril seeds potentiating intracellular tau aggregation. *Alzheimers Res Ther* 2019, 11(1):86.
48. Zhang H, Cao Y, Ma L, Wei Y, Li H: Possible Mechanisms of Tau Spread and Toxicity in Alzheimer's Disease. *Front Cell Dev Biol* 2021, 9:707268.
49. Zhao Z, Nelson AR, Betsholtz C, Zlokovic BV: Establishment and Dysfunction of the Blood-Brain Barrier. *Cell* 2015, 163(5):1064-1078.
50. Greene C, Hanley N, Campbell M: Claudin-5: gatekeeper of neurological function. *Fluids Barriers CNS* 2019, 16(1):3.
51. Armulik A, Genove G, Mae M, Nisancioglu MH, Wallgard E, Niaudet C, He L, Norlin J, Lindblom P, Strittmatter K *et al*: Pericytes regulate the blood-brain barrier. *Nature* 2010, 468(7323):557-561.
52. Alvarez JI, Katayama T, Prat A: Glial influence on the blood brain barrier. *Glia* 2013, 61(12):1939-1958.
53. Jin J, Fang F, Gao W, Chen H, Wen J, Wen X, Chen J: The Structure and Function of the Glycocalyx and Its Connection With Blood-Brain Barrier. *Front Cell Neurosci* 2021, 15:739699.
54. Xu L, Nirwane A, Yao Y: Basement membrane and blood-brain barrier. *Stroke Vasc Neurol* 2019, 4(2):78-82.
55. Zenaro E, Piacentino G, Constantin G: The blood-brain barrier in Alzheimer's disease. *Neurobiol Dis* 2017, 107:41-56.
56. Bourassa P, Tremblay C, Schneider JA, Bennett DA, Calon F: Beta-amyloid pathology in human brain microvessel extracts from the parietal cortex: relation with cerebral amyloid angiopathy and Alzheimer's disease. *Acta Neuropathol* 2019, 137(5):801-823.
57. Wolburg H, Paulus W: Choroid plexus: biology and pathology. *Acta Neuropathol* 2010, 119(1):75-88.
58. Engelhardt B, Vajkoczy P, Weller RO: The movers and shapers in immune privilege of the CNS. *Nat Immunol* 2017, 18(2):123-131.
59. Kemp SF, Creech RH, Horn TR: Glycosylated albumin and transferrin: short-term markers of blood glucose control. *J Pediatr* 1984, 105(3):394-398.
60. MacGillivray RT, Mendez E, Shewale JG, Sinha SK, Lineback-Zins J, Brew K: The primary structure of human serum transferrin. The structures of seven cyanogen bromide fragments and the assembly of the complete structure. *J Biol Chem* 1983, 258(6):3543-3553.
61. Steere AN, Byrne SL, Chasteen ND, Mason AB: Kinetics of iron release from transferrin bound to the transferrin receptor at endosomal pH. *Biochim Biophys Acta* 2012, 1820(3):326-333.

62. Kawabata H: Transferrin and transferrin receptors update. *Free Radic Biol Med* 2019, 133:46-54.
63. Zhang W, Liu QY, Haqqani AS, Leclerc S, Liu Z, Fauteux F, Baumann E, Delaney CE, Ly D, Star AT *et al*: Differential expression of receptors mediating receptor-mediated transcytosis (RMT) in brain microvessels, brain parenchyma and peripheral tissues of the mouse and the human. *Fluids Barriers CNS* 2020, 17(1):47.
64. Luck AN, Mason AB: Transferrin-mediated cellular iron delivery. *Curr Top Membr* 2012, 69:3-35.
65. Johnsen KB, Burkhart A, Thomsen LB, Andresen TL, Moos T: Targeting the transferrin receptor for brain drug delivery. *Prog Neurobiol* 2019, 181:101665.
66. DiSabato DJ, Quan N, Godbout JP: Neuroinflammation: the devil is in the details. *J Neurochem* 2016, 139 Suppl 2:136-153.
67. Ismail R, Parbo P, Madsen LS, Hansen AK, Hansen KV, Schaldemose JL, Kjeldsen PL, Stokholm MG, Gottrup H, Eskildsen SF *et al*: The relationships between neuroinflammation, beta-amyloid and tau deposition in Alzheimer's disease: a longitudinal PET study. *J Neuroinflammation* 2020, 17(1):151.
68. Kinney JW, Bemiller SM, Murtishaw AS, Leisgang AM, Salazar AM, Lamb BT: Inflammation as a central mechanism in Alzheimer's disease. *Alzheimers Dement (N Y)* 2018, 4:575-590.
69. Lee HG, Wheeler MA, Quintana FJ: Function and therapeutic value of astrocytes in neurological diseases. *Nat Rev Drug Discov* 2022.
70. Jessen NA, Munk AS, Lundgaard I, Nedergaard M: The Glymphatic System: A Beginner's Guide. *Neurochem Res* 2015, 40(12):2583-2599.
71. Funato H, Yoshimura M, Yamazaki T, Saido TC, Ito Y, Yokofujita J, Okeda R, Ihara Y: Astrocytes containing amyloid beta-protein (A β)-positive granules are associated with A β 40-positive diffuse plaques in the aged human brain. *Am J Pathol* 1998, 152(4):983-992.
72. Augusto-Oliveira M, Arrifano GP, Lopes-Araujo A, Santos-Sacramento L, Takeda PY, Anthony DC, Malva JO, Crespo-Lopez ME: What Do Microglia Really Do in Healthy Adult Brain? *Cells* 2019, 8(10).
73. Hansen DV, Hanson JE, Sheng M: Microglia in Alzheimer's disease. *J Cell Biol* 2018, 217(2):459-472.
74. Gratuze M, Leyns CEG, Holtzman DM: New insights into the role of TREM2 in Alzheimer's disease. *Mol Neurodegener* 2018, 13(1):66.
75. Ulland TK, Colonna M: TREM2 - a key player in microglial biology and Alzheimer disease. *Nat Rev Neurol* 2018, 14(11):667-675.
76. Carmona S, Zahs K, Wu E, Dakin K, Bras J, Guerreiro R: The role of TREM2 in Alzheimer's disease and other neurodegenerative disorders. *Lancet Neurol* 2018, 17(8):721-730.
77. Song WM, Joshita S, Zhou Y, Ulland TK, Gilfillan S, Colonna M: Humanized TREM2 mice reveal microglia-intrinsic and -extrinsic effects of R47H polymorphism. *J Exp Med* 2018, 215(3):745-760.
78. Naylor S: Biomarkers: current perspectives and future prospects. *Expert Rev Mol Diagn* 2003, 3(5):525-529.

79. Hladky SB, Barrand MA: Mechanisms of fluid movement into, through and out of the brain: evaluation of the evidence. *Fluids Barriers CNS* 2014, 11(1):26.
80. Hansson O, Zetterberg H, Buchhave P, Londos E, Blennow K, Minthon L: Association between CSF biomarkers and incipient Alzheimer's disease in patients with mild cognitive impairment: a follow-up study. *Lancet Neurol* 2006, 5(3):228-234.
81. Blennow K, Zetterberg H, Fagan AM: Fluid biomarkers in Alzheimer disease. *Cold Spring Harb Perspect Med* 2012, 2(9):a006221.
82. Hansson O, Zetterberg H, Buchhave P, Andreasson U, Londos E, Minthon L, Blennow K: Prediction of Alzheimer's disease using the CSF Abeta42/Abeta40 ratio in patients with mild cognitive impairment. *Dement Geriatr Cogn Disord* 2007, 23(5):316-320.
83. Janelidze S, Zetterberg H, Mattsson N, Palmqvist S, Vanderstichele H, Lindberg O, van Westen D, Stomrud E, Minthon L, Blennow K *et al*: CSF Abeta42/Abeta40 and Abeta42/Abeta38 ratios: better diagnostic markers of Alzheimer disease. *Ann Clin Transl Neurol* 2016, 3(3):154-165.
84. Buerger K, Ewers M, Pirttila T, Zinkowski R, Alafuzoff I, Teipel SJ, DeBernardis J, Kerkman D, McCulloch C, Soininen H *et al*: CSF phosphorylated tau protein correlates with neocortical neurofibrillary pathology in Alzheimer's disease. *Brain* 2006, 129(Pt 11):3035-3041.
85. Tapiola T, Alafuzoff I, Herukka SK, Parkkinen L, Hartikainen P, Soininen H, Pirttila T: Cerebrospinal fluid {beta}-amyloid 42 and tau proteins as biomarkers of Alzheimer-type pathologic changes in the brain. *Arch Neurol* 2009, 66(3):382-389.
86. Suarez-Calvet M, Kleinberger G, Araque Caballero MA, Brendel M, Rominger A, Alcolea D, Fortea J, Lleó A, Blesa R, Gispert JD *et al*: sTREM2 cerebrospinal fluid levels are a potential biomarker for microglia activity in early-stage Alzheimer's disease and associate with neuronal injury markers. *EMBO Mol Med* 2016, 8(5):466-476.
87. Fukumoto H, Tennis M, Locascio JJ, Hyman BT, Growdon JH, Irizarry MC: Age but not diagnosis is the main predictor of plasma amyloid beta-protein levels. *Arch Neurol* 2003, 60(7):958-964.
88. Janelidze S, Stomrud E, Palmqvist S, Zetterberg H, van Westen D, Jeromin A, Song L, Hanlon D, Tan Hehir CA, Baker D *et al*: Plasma beta-amyloid in Alzheimer's disease and vascular disease. *Sci Rep* 2016, 6:26801.
89. Nakamura A, Kaneko N, Villemagne VL, Kato T, Doecke J, Dore V, Fowler C, Li QX, Martins R, Rowe C *et al*: High performance plasma amyloid-beta biomarkers for Alzheimer's disease. *Nature* 2018, 554(7691):249-254.
90. Puig KL, Combs CK: Expression and function of APP and its metabolites outside the central nervous system. *Exp Gerontol* 2013, 48(7):608-611.
91. Janelidze S, Mattsson N, Palmqvist S, Smith R, Beach TG, Serrano GE, Chai X, Proctor NK, Eichenlaub U, Zetterberg H *et al*: Plasma P-tau181 in Alzheimer's disease: relationship to other biomarkers, differential diagnosis, neuropathology and longitudinal progression to Alzheimer's dementia. *Nat Med* 2020, 26(3):379-386.

92. Lantero Rodriguez J, Karikari TK, Suarez-Calvet M, Troakes C, King A, Emersic A, Aarsland D, Hye A, Zetterberg H, Blennow K *et al*: Plasma p-tau181 accurately predicts Alzheimer's disease pathology at least 8 years prior to post-mortem and improves the clinical characterisation of cognitive decline. *Acta Neuropathol* 2020, 140(3):267-278.
93. Palmqvist S, Janelidze S, Quiroz YT, Zetterberg H, Lopera F, Stomrud E, Su Y, Chen Y, Serrano GE, Leuzy A *et al*: Discriminative Accuracy of Plasma Phospho-tau217 for Alzheimer Disease vs Other Neurodegenerative Disorders. *JAMA* 2020, 324(8):772-781.
94. Klunk WE, Engler H, Nordberg A, Wang Y, Blomqvist G, Holt DP, Bergstrom M, Savitcheva I, Huang GF, Estrada S *et al*: Imaging brain amyloid in Alzheimer's disease with Pittsburgh Compound-B. *Ann Neurol* 2004, 55(3):306-319.
95. Wu C, Bowers MT, Shea JE: On the origin of the stronger binding of PIB over thioflavin T to protofibrils of the Alzheimer amyloid-beta peptide: a molecular dynamics study. *Biophys J* 2011, 100(5):1316-1324.
96. van Waarde A, Marcolini S, de Deyn PP, Dierckx R: PET Agents in Dementia: An Overview. *Semin Nucl Med* 2021, 51(3):196-229.
97. Engler H, Forsberg A, Almkvist O, Blomqvist G, Larsson E, Savitcheva I, Wall A, Ringheim A, Langstrom B, Nordberg A: Two-year follow-up of amyloid deposition in patients with Alzheimer's disease. *Brain* 2006, 129(Pt 11):2856-2866.
98. Palmqvist S, Zetterberg H, Mattsson N, Johansson P, Alzheimer's Disease Neuroimaging I, Minthon L, Blennow K, Olsson M, Hansson O, Swedish Bio FSG: Detailed comparison of amyloid PET and CSF biomarkers for identifying early Alzheimer disease. *Neurology* 2015, 85(14):1240-1249.
99. Fodero-Tavoletti MT, Okamura N, Furumoto S, Mulligan RS, Connor AR, McLean CA, Cao D, Rigopoulos A, Cartwright GA, O'Keefe G *et al*: 18F-THK523: a novel in vivo tau imaging ligand for Alzheimer's disease. *Brain* 2011, 134(Pt 4):1089-1100.
100. Murugan NA, Chiotis K, Rodriguez-Vieitez E, Lemoine L, Agren H, Nordberg A: Cross-interaction of tau PET tracers with monoamine oxidase B: evidence from in silico modelling and in vivo imaging. *Eur J Nucl Med Mol Imaging* 2019, 46(6):1369-1382.
101. Villemagne VL, Furumoto S, Fodero-Tavoletti MT, Mulligan RS, Hodges J, Harada R, Yates P, Piguet O, Pejoska S, Dore V *et al*: In vivo evaluation of a novel tau imaging tracer for Alzheimer's disease. *Eur J Nucl Med Mol Imaging* 2014, 41(5):816-826.
102. Marquie M, Normandin MD, Vanderburg CR, Costantino IM, Bien EA, Rycyna LG, Klunk WE, Mathis CA, Ikonomovic MD, Debnath ML *et al*: Validating novel tau positron emission tomography tracer [F-18]-AV-1451 (T807) on postmortem brain tissue. *Ann Neurol* 2015, 78(5):787-800.
103. Lowe VJ, Curran G, Fang P, Liesinger AM, Josephs KA, Parisi JE, Kantarci K, Boeve BF, Pandey MK, Bruinsma T *et al*: An autoradiographic evaluation of AV-1451 Tau PET in dementia. *Acta Neuropathol Commun* 2016, 4(1):58.

104. Bejanin A, Schonhaut DR, La Joie R, Kramer JH, Baker SL, Sosa N, Ayakta N, Cantwell A, Janabi M, Lauriola M *et al*: Tau pathology and neurodegeneration contribute to cognitive impairment in Alzheimer's disease. *Brain* 2017, 140(12):3286-3300.
105. Vermeiren C, Motte P, Viot D, Mairet-Coello G, Courade JP, Citron M, Mercier J, Hannestad J, Gillard M: The tau positron-emission tomography tracer AV-1451 binds with similar affinities to tau fibrils and monoamine oxidases. *Mov Disord* 2018, 33(2):273-281.
106. Tago T, Toyohara J, Harada R, Furumoto S, Okamura N, Kudo Y, Takahashi-Fujigasaki J, Murayama S, Ishii K: Characterization of the binding of tau imaging ligands to melanin-containing cells: putative off-target-binding site. *Ann Nucl Med* 2019, 33(6):375-382.
107. Coakeley S, Cho SS, Koshimori Y, Rusjan P, Ghadery C, Kim J, Lang AE, Houle S, Strafella AP: [(18F)AV-1451 binding to neuromelanin in the substantia nigra in PD and PSP. *Brain Struct Funct* 2018, 223(2):589-595.
108. Werry EL, Bright FM, Piguet O, Ittner LM, Halliday GM, Hodges JR, Kiernan MC, Loy CT, Kril JJ, Kassiou M: Recent Developments in TSPO PET Imaging as A Biomarker of Neuroinflammation in Neurodegenerative Disorders. *Int J Mol Sci* 2019, 20(13).
109. Parbo P, Ismail R, Hansen KV, Amidi A, Marup FH, Gottrup H, Braendgaard H, Eriksson BO, Eskildsen SF, Lund TE *et al*: Brain inflammation accompanies amyloid in the majority of mild cognitive impairment cases due to Alzheimer's disease. *Brain* 2017, 140(7):2002-2011.
110. Vivash L, O'Brien TJ: Imaging Microglial Activation with TSPO PET: Lighting Up Neurologic Diseases? *J Nucl Med* 2016, 57(2):165-168.
111. Mizrahi R, Rusjan PM, Kennedy J, Pollock B, Mulsant B, Suridjan I, De Luca V, Wilson AA, Houle S: Translocator protein (18 kDa) polymorphism (rs6971) explains in-vivo brain binding affinity of the PET radioligand [(18F)-FEPPA. *J Cereb Blood Flow Metab* 2012, 32(6):968-972.
112. Schenk D, Barbour R, Dunn W, Gordon G, Grajeda H, Guido T, Hu K, Huang J, Johnson-Wood K, Khan K *et al*: Immunization with amyloid-beta attenuates Alzheimer-disease-like pathology in the PDAPP mouse. *Nature* 1999, 400(6740):173-177.
113. Gilman S, Koller M, Black RS, Jenkins L, Griffith SG, Fox NC, Eisner L, Kirby L, Rovira MB, Forette F *et al*: Clinical effects of Abeta immunization (AN1792) in patients with AD in an interrupted trial. *Neurology* 2005, 64(9):1553-1562.
114. Cribbs DH, Ghochikyan A, Vasilevko V, Tran M, Petrushina I, Sadzikava N, Babikyan D, Kesslak P, Kieber-Emmons T, Cotman CW *et al*: Adjuvant-dependent modulation of Th1 and Th2 responses to immunization with beta-amyloid. *Int Immunol* 2003, 15(4):505-514.
115. Winblad B, Graf A, Riviere ME, Andreasen N, Ryan JM: Active immunotherapy options for Alzheimer's disease. *Alzheimers Res Ther* 2014, 6(1):7.
116. Mantile F, Prisco A: Vaccination against beta-Amyloid as a Strategy for the Prevention of Alzheimer's Disease. *Biology (Basel)* 2020, 9(12).

117. Sandberg A, Luheshi LM, Sollvander S, Pereira de Barros T, Macao B, Knowles TP, Biverstal H, Lendel C, Ekholm-Petterson F, Dubnovitsky A *et al*: Stabilization of neurotoxic Alzheimer amyloid-beta oligomers by protein engineering. *Proc Natl Acad Sci U S A* 2010, 107(35):15595-15600.
118. ALZ-101 [<https://www.alzforum.org/therapeutics/alz-101>]
119. Ciabattini A, Nardini C, Santoro F, Garagnani P, Franceschi C, Medaglini D: Vaccination in the elderly: The challenge of immune changes with aging. *Semin Immunol* 2018, 40:83-94.
120. Johnson-Wood K, Lee M, Motter R, Hu K, Gordon G, Barbour R, Khan K, Gordon M, Tan H, Games D *et al*: Amyloid precursor protein processing and A beta42 deposition in a transgenic mouse model of Alzheimer disease. *Proc Natl Acad Sci U S A* 1997, 94(4):1550-1555.
121. DeMattos RB, Bales KR, Cummins DJ, Dodart JC, Paul SM, Holtzman DM: Peripheral anti-A beta antibody alters CNS and plasma A beta clearance and decreases brain A beta burden in a mouse model of Alzheimer's disease. *Proc Natl Acad Sci U S A* 2001, 98(15):8850-8855.
122. Bohrmann B, Baumann K, Benz J, Gerber F, Huber W, Knoflach F, Messer J, Oroszlan K, Rauchenberger R, Richter WF *et al*: Gantenerumab: a novel human anti-Abeta antibody demonstrates sustained cerebral amyloid-beta binding and elicits cell-mediated removal of human amyloid-beta. *J Alzheimers Dis* 2012, 28(1):49-69.
123. Demattos RB, Lu J, Tang Y, Racke MM, DeLong CA, Tzaferis JA, Hole JT, Forster BM, McDonnell PC, Liu F *et al*: A plaque-specific antibody clears existing beta-amyloid plaques in Alzheimer's disease mice. *Neuron* 2012, 76(5):908-920.
124. Sevigny J, Chiao P, Bussiere T, Weinreb PH, Williams L, Maier M, Dunstan R, Salloway S, Chen T, Ling Y *et al*: The antibody aducanumab reduces Abeta plaques in Alzheimer's disease. *Nature* 2016, 537(7618):50-56.
125. Lord A, Gumucio A, Englund H, Sehlin D, Sundquist VS, Soderberg L, Moller C, Gellerfors P, Lannfelt L, Pettersson FE *et al*: An amyloid-beta protofibril-selective antibody prevents amyloid formation in a mouse model of Alzheimer's disease. *Neurobiol Dis* 2009, 36(3):425-434.
126. Salloway S, Sperling R, Fox NC, Blennow K, Klunk W, Raskind M, Sabbagh M, Honig LS, Porsteinsson AP, Ferris S *et al*: Two phase 3 trials of bapineuzumab in mild-to-moderate Alzheimer's disease. *N Engl J Med* 2014, 370(4):322-333.
127. Arrighi HM, Barakos J, Barkhof F, Tampieri D, Jack C, Jr., Melancon D, Morris K, Ketter N, Liu E, Brashear HR: Amyloid-related imaging abnormalities-haemosiderin (ARIA-H) in patients with Alzheimer's disease treated with bapineuzumab: a historical, prospective secondary analysis. *J Neurol Neurosurg Psychiatry* 2016, 87(1):106-112.
128. Laskowitz DT, Kolls BJ: A phase 2 multiple ascending dose trial of bapineuzumab in mild to moderate Alzheimer disease. *Neurology* 2010, 74(24):2026; author reply 2026-2027.
129. Ferrero J, Williams L, Stella H, Leitermann K, Mikulskis A, O'Gorman J, Sevigny J: First-in-human, double-blind, placebo-controlled, single-dose escalation study of aducanumab (BIIB037) in mild-to-moderate Alzheimer's disease. *Alzheimers Dement (N Y)* 2016, 2(3):169-176.

130. Knopman DS, Jones DT, Greicius MD: Failure to demonstrate efficacy of aducanumab: An analysis of the EMERGE and ENGAGE trials as reported by Biogen, December 2019. *Alzheimers Dement* 2021, 17(4):696-701.
131. Huang LK, Chao SP, Hu CJ: Clinical trials of new drugs for Alzheimer disease. *J Biomed Sci* 2020, 27(1):18.
132. Lannfelt L, Moller C, Basun H, Osswald G, Sehlin D, Satlin A, Logovinsky V, Gellerfors P: Perspectives on future Alzheimer therapies: amyloid-beta protofibrils - a new target for immunotherapy with BAN2401 in Alzheimer's disease. *Alzheimers Res Ther* 2014, 6(2):16.
133. Englund H, Sehlin D, Johansson AS, Nilsson LN, Gellerfors P, Paulie S, Lannfelt L, Pettersson FE: Sensitive ELISA detection of amyloid-beta protofibrils in biological samples. *J Neurochem* 2007, 103(1):334-345.
134. Swanson C: Treatment of Early AD subjects with BAN2401, an Anti-A β Protofibril Monoclonal Antibody, Significantly Clears Amyloid Plaque and Reduces Clinical Decline. In: *AAIC18*. Chicago; 2018.
135. A Study to Confirm Safety and Efficacy of Lecanemab in Participants With Early Alzheimer's Disease. In.
136. Bard F, Cannon C, Barbour R, Burke RL, Games D, Grajeda H, Guido T, Hu K, Huang J, Johnson-Wood K *et al*: Peripherally administered antibodies against amyloid beta-peptide enter the central nervous system and reduce pathology in a mouse model of Alzheimer disease. *Nat Med* 2000, 6(8):916-919.
137. Pardridge WM: CSF, blood-brain barrier, and brain drug delivery. *Expert Opin Drug Deliv* 2016, 13(7):963-975.
138. Cosolo WC, Martinello P, Louis WJ, Christophidis N: Blood-brain barrier disruption using mannitol: time course and electron microscopy studies. *Am J Physiol* 1989, 256(2 Pt 2):R443-447.
139. Abrahao A, Meng Y, Llinas M, Huang Y, Hamani C, Mainprize T, Aubert I, Heyn C, Black SE, Hynynen K *et al*: First-in-human trial of blood-brain barrier opening in amyotrophic lateral sclerosis using MR-guided focused ultrasound. *Nat Commun* 2019, 10(1):4373.
140. Shen Y, Guo J, Chen G, Chin CT, Chen X, Chen J, Wang F, Chen S, Dan G: Delivery of Liposomes with Different Sizes to Mice Brain after Sonication by Focused Ultrasound in the Presence of Microbubbles. *Ultrasound Med Biol* 2016, 42(7):1499-1511.
141. Lipsman N, Meng Y, Bethune AJ, Huang Y, Lam B, Masellis M, Herrmann N, Heyn C, Aubert I, Boutet A *et al*: Blood-brain barrier opening in Alzheimer's disease using MR-guided focused ultrasound. *Nat Commun* 2018, 9(1):2336.
142. Pardridge WM, Kang YS, Buciak JL, Yang J: Human insulin receptor monoclonal antibody undergoes high affinity binding to human brain capillaries in vitro and rapid transcytosis through the blood-brain barrier in vivo in the primate. *Pharm Res* 1995, 12(6):807-816.
143. Alata W, Yogi A, Brunette E, Delaney CE, van Faassen H, Hussack G, Iqbal U, Kemmerich K, Haqqani AS, Moreno MJ *et al*: Targeting insulin-like growth factor-1 receptor (IGF1R) for brain delivery of biologics. *FASEB J* 2022, 36(3):e22208.

144. Webster CI, Caram-Salas N, Haqqani AS, Thom G, Brown L, Rennie K, Yogi A, Costain W, Brunette E, Stanimirovic DB: Brain penetration, target engagement, and disposition of the blood-brain barrier-crossing bispecific antibody antagonist of metabotropic glutamate receptor type 1. *FASEB J* 2016, 30(5):1927-1940.
145. Abulrob A, Sprong H, Van Bergen en Henegouwen P, Stanimirovic D: The blood-brain barrier transmigration single domain antibody: mechanisms of transport and antigenic epitopes in human brain endothelial cells. *J Neurochem* 2005, 95(4):1201-1214.
146. Friden PM, Walus LR, Musso GF, Taylor MA, Malfroy B, Starzyk RM: Anti-transferrin receptor antibody and antibody-drug conjugates cross the blood-brain barrier. *Proc Natl Acad Sci U S A* 1991, 88(11):4771-4775.
147. Boado RJ, Zhou QH, Lu JZ, Hui EK, Pardridge WM: Pharmacokinetics and brain uptake of a genetically engineered bifunctional fusion antibody targeting the mouse transferrin receptor. *Mol Pharm* 2010, 7(1):237-244.
148. Pardridge WM: Molecular Trojan horses for blood-brain barrier drug delivery. *Curr Opin Pharmacol* 2006, 6(5):494-500.
149. Haqqani AS, Thom G, Burrell M, Delaney CE, Brunette E, Baumann E, Sodja C, Jezierski A, Webster C, Stanimirovic DB: Intracellular sorting and transcytosis of the rat transferrin receptor antibody OX26 across the blood-brain barrier in vitro is dependent on its binding affinity. *J Neurochem* 2018, 146(6):735-752.
150. Thom G, Burrell M, Haqqani AS, Yogi A, Lessard E, Brunette E, Delaney C, Baumann E, Callaghan D, Rodrigo N *et al*: Enhanced Delivery of Galanin Conjugates to the Brain through Bioengineering of the Anti-Transferrin Receptor Antibody OX26. *Mol Pharm* 2018, 15(4):1420-1431.
151. Yu YJ, Zhang Y, Kenrick M, Hoyte K, Luk W, Lu Y, Atwal J, Elliott JM, Prabhu S, Watts RJ *et al*: Boosting brain uptake of a therapeutic antibody by reducing its affinity for a transcytosis target. *Sci Transl Med* 2011, 3(84):84ra44.
152. Niewoehner J, Bohrmann B, Collin L, Urich E, Sade H, Maier P, Rueger P, Stracke JO, Lau W, Tissot AC *et al*: Increased brain penetration and potency of a therapeutic antibody using a monovalent molecular shuttle. *Neuron* 2014, 81(1):49-60.
153. Hultqvist G, Syvanen S, Fang XT, Lannfelt L, Sehlin D: Bivalent Brain Shuttle Increases Antibody Uptake by Monovalent Binding to the Transferrin Receptor. *Theranostics* 2017, 7(2):308-318.
154. Sehlin D, Syvanen S, faculty M: Engineered antibodies: new possibilities for brain PET? *Eur J Nucl Med Mol Imaging* 2019, 46(13):2848-2858.
155. Fang XT, Hultqvist G, Meier SR, Antoni G, Sehlin D, Syvanen S: High detection sensitivity with antibody-based PET radioligand for amyloid beta in brain. *Neuroimage* 2019, 184:881-888.
156. Sehlin D, Fang XT, Cato L, Antoni G, Lannfelt L, Syvanen S: Antibody-based PET imaging of amyloid beta in mouse models of Alzheimer's disease. *Nat Commun* 2016, 7:10759.
157. Syvanen S, Fang XT, Hultqvist G, Meier SR, Lannfelt L, Sehlin D: A bispecific Tribody PET radioligand for visualization of amyloid-beta protofibrils - a new concept for neuroimaging. *Neuroimage* 2017, 148:55-63.

158. Weber F, Bohrmann B, Niewoehner J, Fischer JAA, Rueger P, Tiefenthaler G, Moelleken J, Bujotzek A, Brady K, Singer T *et al*: Brain Shuttle Antibody for Alzheimer's Disease with Attenuated Peripheral Effector Function due to an Inverted Binding Mode. *Cell Rep* 2018, 22(1):149-162.
159. Bard F, Barbour R, Cannon C, Carretto R, Fox M, Games D, Guido T, Hoenow K, Hu K, Johnson-Wood K *et al*: Epitope and isotype specificities of antibodies to beta -amyloid peptide for protection against Alzheimer's disease-like neuropathology. *Proc Natl Acad Sci U S A* 2003, 100(4):2023-2028.
160. Abbott NJ, Pizzo ME, Preston JE, Janigro D, Thorne RG: The role of brain barriers in fluid movement in the CNS: is there a 'glymphatic' system? *Acta Neuropathol* 2018, 135(3):387-407.
161. Meier SR, Syvanen S, Hultqvist G, Fang XT, Roshanbin S, Lannfelt L, Neumann U, Sehlin D: Antibody-based in vivo PET imaging detects amyloid-beta reduction in Alzheimer transgenic mice after BACE-1 inhibition. *J Nucl Med* 2018.
162. Meier SR, Sehlin D, Roshanbin S, Falk VL, Saito T, Saido TC, Neumann U, Rokka J, Eriksson J, Syvanen S: (11)C-PiB and (124)I-Antibody PET Provide Differing Estimates of Brain Amyloid-beta After Therapeutic Intervention. *J Nucl Med* 2022, 63(2):302-309.
163. Schellekens H: Immunogenicity of therapeutic proteins: clinical implications and future prospects. *Clin Ther* 2002, 24(11):1720-1740; discussion 1719.
164. Gunn GR, 3rd, Sealey DC, Jamali F, Meibohm B, Ghosh S, Shankar G: From the bench to clinical practice: understanding the challenges and uncertainties in immunogenicity testing for biopharmaceuticals. *Clin Exp Immunol* 2016, 184(2):137-146.
165. Rosenberg AS: Effects of protein aggregates: an immunologic perspective. *AAPS J* 2006, 8(3):E501-507.
166. Neeffjes J, Jongsma ML, Paul P, Bakke O: Towards a systems understanding of MHC class I and MHC class II antigen presentation. *Nat Rev Immunol* 2011, 11(12):823-836.
167. Krishna M, Nadler SG: Immunogenicity to Biotherapeutics - The Role of Anti-drug Immune Complexes. *Front Immunol* 2016, 7:21.
168. Lord A, Kalimo H, Eckman C, Zhang XQ, Lannfelt L, Nilsson LN: The Arctic Alzheimer mutation facilitates early intraneuronal Abeta aggregation and senile plaque formation in transgenic mice. *Neurobiol Aging* 2006, 27(1):67-77.
169. Lillehaug S, Syverstad GH, Nilsson LN, Bjaalie JG, Leergaard TB, Torp R: Brainwide distribution and variance of amyloid-beta deposits in tg-ArcSwe mice. *Neurobiol Aging* 2014, 35(3):556-564.
170. Lord A, Englund H, Soderberg L, Tucker S, Clausen F, Hillered L, Gordon M, Morgan D, Lannfelt L, Pettersson FE *et al*: Amyloid-beta protofibril levels correlate with spatial learning in Arctic Alzheimer's disease transgenic mice. *FEBS J* 2009, 276(4):995-1006.
171. Fang XT, Sehlin D, Lannfelt L, Syvanen S, Hultqvist G: Efficient and inexpensive transient expression of multispecific multivalent antibodies in Expi293 cells. *Biol Proced Online* 2017, 19:11.

172. Basu S, Kwee TC, Surti S, Akin EA, Yoo D, Alavi A: Fundamentals of PET and PET/CT imaging. *Ann N Y Acad Sci* 2011, 1228:1-18.
173. Cherry S SJ, Phelps M: Physics in Nuclear Medicine, 4th edn: Elsevier; 2012.
174. Groch MW, Erwin WD: SPECT in the year 2000: basic principles. *J Nucl Med Technol* 2000, 28(4):233-244.
175. Van Audenhaege K, Van Holen R, Vandenberghe S, Vanhove C, Metzler SD, Moore SC: Review of SPECT collimator selection, optimization, and fabrication for clinical and preclinical imaging. *Med Phys* 2015, 42(8):4796-4813.
176. Partridge WM: Treatment of Alzheimer's Disease and Blood-Brain Barrier Drug Delivery. *Pharmaceuticals (Basel)* 2020, 13(11).
177. Pizzo ME, Wolak DJ, Kumar NN, Brunette E, Brunnquell CL, Hannocks MJ, Abbott NJ, Meyerand ME, Sorokin L, Stanimirovic DB *et al*: Intrathecal antibody distribution in the rat brain: surface diffusion, perivascular transport and osmotic enhancement of delivery. *J Physiol* 2018, 596(3):445-475.
178. Gustavsson T, Syvanen S, O'Callaghan P, Sehlin D: SPECT imaging of distribution and retention of a brain-penetrating bispecific amyloid-beta antibody in a mouse model of Alzheimer's disease. *Transl Neurodegener* 2020, 9(1):37.
179. Faresjo R, Bonvicini G, Fang XT, Aguilar X, Sehlin D, Syvanen S: Brain pharmacokinetics of two BBB penetrating bispecific antibodies of different size. *Fluids Barriers CNS* 2021, 18(1):26.
180. Moos T, Oates PS, Morgan EH: Expression of the neuronal transferrin receptor is age dependent and susceptible to iron deficiency. *J Comp Neurol* 1998, 398(3):420-430.
181. Moos T, Oates PS, Morgan EH: Iron-independent neuronal expression of transferrin receptor mRNA in the rat. *Brain Res Mol Brain Res* 1999, 72(2):231-234.
182. Syvanen S, Hultqvist G, Gustavsson T, Gumucio A, Laudon H, Soderberg L, Ingelsson M, Lannfelt L, Sehlin D: Efficient clearance of Abeta protofibrils in AbetaPP-transgenic mice treated with a brain-penetrating bifunctional antibody. *Alzheimers Res Ther* 2018, 10(1):49.
183. Sperling R, Salloway S, Brooks DJ, Tampieri D, Barakos J, Fox NC, Raskind M, Sabbagh M, Honig LS, Porsteinsson AP *et al*: Amyloid-related imaging abnormalities in patients with Alzheimer's disease treated with bapineuzumab: a retrospective analysis. *Lancet Neurol* 2012, 11(3):241-249.
184. Brainshuttle AD: A Multiple Ascending Dose Study to Investigate the Safety, Tolerability, Pharmacokinetics, and Pharmacodynamics of RO7126209 Following Intravenous Infusion in Participants With Prodromal or Mild to Moderate Alzheimer's Disease. In.

Acta Universitatis Upsaliensis

*Digital Comprehensive Summaries of Uppsala Dissertations
from the Faculty of Medicine 1817*

Editor: The Dean of the Faculty of Medicine

A doctoral dissertation from the Faculty of Medicine, Uppsala University, is usually a summary of a number of papers. A few copies of the complete dissertation are kept at major Swedish research libraries, while the summary alone is distributed internationally through the series Digital Comprehensive Summaries of Uppsala Dissertations from the Faculty of Medicine. (Prior to January, 2005, the series was published under the title “Comprehensive Summaries of Uppsala Dissertations from the Faculty of Medicine”.)

Distribution: publications.uu.se
urn:nbn:se:uu:diva-469103



ACTA
UNIVERSITATIS
UPSALIENSIS
UPPSALA
2022